# CHARACTERISATION AND INTERACTION OF MIXED ALKALINE CLAYS AND MORINGA SEEDS WITH HEAVY METALS IN CONTAMINATED WATER

Samson Mkali Idruss Sajidu, BSc (Mlw), MPhil (Camb)

A Thesis submitted to the University of Malawi in partial fulfilment of the requirements for the Degree of Doctor of Philosophy in Chemistry

Chemistry Department
April 2008

#### **DECLARATION**

I declare that the thesis submitted herein is my original work except for the cited literature, and has not been submitted for any other awards in this University or elsewhere.

Signature of the candidate			
Samson M.I. Sajidu:			
Date:			
We hereby declare that this thesis is from submitted this day with our approval.	the student's own effort and that it has been		
Associate Professor Wellington R.L. Masamb (Main supervisor, University of Malawi)	pa Date		
Professor Ingmar Persson (Supervisor, Swedish University of Agricultu	Date ral Sciences)		
Dr. Denis Kayambazinthu (Supervisor, Forestry Research Institute of Management)	Date alawi)		
Professor John D.K. Saka	Date		
(Internal Examiner)			
Head of Chemistry Department	Date		

#### ACKNOWLEDGMENTS

I wish to thank all members of my supervisory team: Associate Professor W.R.L Masamba (University of Malawi), Professor I. Persson (Swedish University of Agricultural Sciences), Professor E. Henry (Deceased), and Dr D. Kayambazinthu (Forestry Research Institute of Malawi) for all their time and guidance during this work. I also would like to thank all staff of the Chemistry Department laboratory, Chancellor College and the City of Blantyre Pollution Control Office (Mr S. Kuyeli in particular) for their technical support during wastewater sampling and Professor J.D.K. Saka and M. Monjerezi for their moral support.

Special thanks to my wife Rachel, my son Tujaliwe and my mother Mariam Apiti Idruss, for their encouragement and support particularly during my stay in Sweden. I also appreciate the encouragement and support from my late grandmother Apiti Kasinde, Uncle Fix Idruss and Cousin Elias Sajidu.

I would like to thank the International Program in Chemical Sciences (IPICS) through the Malawi water project (code MAW:02) for providing studentship/fellowship that enabled my work to be done both in Malawi and Sweden. Special thanks to Malin Åkerblom (former director of IPICS), Peter Sundin (IPICS director), Linnea Sjöblom (IPICS Assistant director) and Hossein Aminaey for their moral support during my time in Sweden. Tack så mycket!!

Finally, I would like to thank God, the Most Gracious, and the Most Merciful for all the blessings.

#### **ABSTRACT**

Surface waters in many cities are known to be highly polluted due to, among other reasons, incompletely treated municipal and industrial wastewaters that are discharged into streams. This thesis concerns (i) some recent physicochemical water quality data in streams (Limbe, Mudi and Nasolo) and wastewater treatment plants (WWTP) (Limbe WWTP, Soche WWTP) in Blantyre City in Malawi and (ii) heavy metal sorption using alkaline mixed clay minerals, *Moringa oleifera* and *Moringa stenopetala* seed extracts of water and sodium chloride.

The levels of lead, cadmium, iron, manganese, zinc, chromium and nickel were much higher than the World Health safe limits for drinking water in all the sampled streams which passed through industrial areas. Although the nitrates and sulphates levels at all sampling points were lower than the safe limits for drinking water of 50 mg/L and 250 mg/L respectively, the phosphate levels were significantly above the safe limit (0.5 mg/L). The biochemical oxygen demand (BOD<sub>5</sub>) was also above the World Health Organisation limit (20 mg/L) at all sites except Mudi and Limbe streams before passing through industrial areas; thus, streams in the city are significantly polluted.

Mixed alkaline clays from Tundulu area in Malawi have shown great potential in sorbing chromium(III), copper(II), zinc(II), cadmium(II), mercury(II) and lead(II) cations within characteristic pH ranges. Using an initial total metal concentrations of about 5 mg/L and clay dose of 0.015g per 10.5 ml of metal solution chromium(III) sorption occurred from pH of 3 to complete removal at pH 5. Complete removal of zinc(II) occurred at pH above 7 while copper(II) was sorbed at pH between 4 and 6.8. The removals of cadmium(II) and lead(II) were achieved at pH between 6 and 9, and >7.7 respectively where as the removal of mercury(II) was pH independent, ranging from 30 to 60% removal. Qualitative mineralogical characterisation of the mixed clays by Powder X-Ray Diffraction (PXRD) revealed presence of illite, distorted kaolinite, mixed layer minerals and non-clay mineral carbonate fluoroapatite. The pH point of zero charge was above 9.6. Extended X-ray Absorption Fine Structure (EXAFS) analyses of the metal sorbed clays revealed that oxygen atoms occupy the first coordination shells in all the studied metals. The metal species on the clay mineral surfaces seem therefore to be hydrolyzed as adsorbates and/or precipitates.

Crude water and sodium chloride extracts of partially defatted powder of *Moringa stenopetala* (MS) and *oleifera* (MO) showed complete removal of chromium(III), copper(II), zinc(II) and cadmium(II) from single ion solution at initial metal concentrations of about 4 mg/L at different pH ranges for each metal. Using proton nuclear magnetic resonance, the *Moringa* extracts showed clear presence of amide (-CO-N-H), benzenoid (Ar-H), saturated alkyl and unsaturated fragments in both MS and MO. EXAFS measurements of the metal rich *Moringa* extracts indicated bonding between the metals and the oxygens of carboxylate and amide groups.

## TABLE OF CONTENTS

Declaration	i
Acknowledgments	ii
Abstract	iii
Table of contents	v
List of Figures	viii
List of Tables	ix
Abbreviations and symbols	X
Appendices	xi
1. INTRODUCTION	1
1.1 Overview	1
1.2 Conventional heavy metal removal from water and wastewater 1.2.1 Chemical precipitation 1.2.2 Ion exchange 1.2.3 Solvent extraction 1.2.4 Adsorption and sand filtration	4 5
1.3 Low-cost methods for heavy metal remediation  1.3.1 Use of natural clay adsorbents  1.3.2 Uses of <i>Moringa</i> seed powder.	7
2. GENERAL AND SPECIFIC OBJECTIVES	14
3. METHODOLOGY	16
3.1 Physicochemical quality of water and wastewater in Blantyre	16
sulphates and biochemical oxygen demand	23
3.1.2.4 pH determination	24

	3.1.2	.5 Determination of total dissolved solids (TDS)	24
	3.1.2	.6 Determination of BOD <sub>5</sub>	24
3	.1.3	Theoretical description of analysis of metal ions by atomic absorption	
		spectroscopy	25
	3.1.3	.1 Sample digestion prior to metal ion determination	
		.2 Determination of metal ions	
3	.1.4	Sources of clay samples and brief description of purification procedures	
		.1 Removal of carbonates	
		.2 Removal of iron oxides	
		.3 Removal of organic matter	
		.4 Fractionation of the clay	
3	.1.5	Brief theory of qualitative mineralogical analysis using Powder X-Ray Diffra	
		(PXRD)	
	3.1.5	.1 Powder X-ray diffraction of the clay samples	
3	.1.6	· · · · · · · · · · · · · · · · · · ·	
		.1 Preparation of 0.5 M copper bisethylenediamine	
		.2 CEC determination.	
3	.1.7	Brief theory of acid-base properties of the clay	
		.1 Potentiometric titrations	
3	.1.8		
		.1 Preparation of metal solutions	
		.2 Metal adsorption	
3	.1.9	Heavy metal uptake mechanism using Extended X-Ray Absorption Fine Stru	
	- 1,	(EXAFS) spectroscopy (background theory)	
	3.1.9	.1 EXAFS sample preparation	
		.2 EXAFS Data collection	
		.3 EXAFS Data analysis	
3	.1.10	Sources of <i>Moringa</i> seeds.	
	.1.11	Preparation and characterisation of the <i>Moringa</i> seeds for heavy metal remov	
		experiments	
3	.1.12	pH profile studies for chromium(III), copper(II), zinc(II) and cadmium(II) so	
		F F(),(),()()	
4.	DE	SULTS AND DISCUSSION	5.4
4.	KE	SULTS AND DISCUSSION	34
4.1	On	ality of water from streams and wastewater treatment plants of Blantyre City	
т.1		per I)	54
4	.1.1	Concentrations/values of pH, total dissolved solids (TDS) and biochemical of	
7	.1.1	demand (BOD <sub>5</sub> )	
4	.1.2	Concentrations of metal cations	
	.1.3	Concentrations of nitrates and phosphates	
7	.1.3	Concentrations of intraces and phosphates	00
4.2	Ch	aracterisation and metal sorption studies of the mixed alkaline clays (Paper II	and
4		Clay characterisation	

4.2	2.2 Effect of pH on metal sorption by the mixed alkaline clay and structural determination	64
4.3	Sorption of heavy metal cations in crude water and sodium chloride extracts of <i>Moringa oleifera</i> and <i>stenopetala</i> (Papers IV and V)	66
5.	PRACTICAL APPLICATIONS OF THE WORK, LIMITATIONS, FUTURE RESEARCH AND CONCLUSIONS	69
REF	ERENCES	71
APP	ENDICES	87

# **List of Figures**

Figure 1	Silicon tetrahedron and aluminium octahedron	7
Figure 2	Seeds of M. oleifera and M. stenopetala	12
Figure 3	Sampling sites in the City of Blantyre	18
Figure 4	Photo of water sampling in Nasolo river	19
Figure 5	Photo of part of Limbe wastewater treatment plant	19
Figure 6	Schematic diagram of atomic absorption spectroscopy instrumental set up	27
Figure 7	Path difference between reflections from successive planes (Brags law)	32
Figure 8	A (210) Miller plane of cubic crystal system	33
Figure 9	An example of a PXRD plot	34
Figure 10	Cr(III) K-edge spectrum of chromium(III) sorbed clays	46
Figure 11	Extraction of EXAFS oscillation from raw data	49
Figure 12	PXRD pattern for raw and purified clays $(5 - 30.2\theta \text{ diffraction angles})$	63
Figure 13	PXRD pattern for raw and purified clays $(31 - 60\ 2\theta\ diffraction\ angles)$	63

## **List of Tables**

Table 1 Cation: oxygen radius ratio for various common ions	8
Table 2 Identification of the three most intense reflections in a PXRD plot	34
Table 3 A section of crystallographic data for corundum from the Mineral Database	35
Table 4 Calculation of $pK_{a_1 app.}$	41
Table 5 Calculation of $pK_{a_2 app.}$	41
Table 6 Metal speciation in stock solution calculated by Visual MINITEQ program	44
Table 7 Concentrations of metal cations in water samples	55
Table 8 Mean values/concentrations of pH, phosphates, nitrates, TDS and BOD	56

#### Abbreviations and symbols

≡SOH clay mineral surface with ≡S representing the surface and OH the attached

hydroxyl group

BOD<sub>5</sub> biochemical oxygen demand after 5 days

CEC cation exchange capacity

DEHPA bis(2-ethyl-hexyl) phosphoric acid

DMSO dimethyl sulfoxide

EXAFS extended X-ray absorption fine structure

HAP Hydroxyapatite

ICDD/JCPDS International Centre for Diffraction Data/Joint Committee on Powder

**Diffraction Standards** 

K<sup>s</sup><sub>a intr</sub> intrinsic acidty constant

MO Moringa oleifera

MOC-DW Moringa oleifera crude extracts of water

MOC-SC *Moringa oleifera* crude extracts of sodium chloride

MS Moringa stenopetala

MSC-DW Moringa stenopetala crude extracts of water

MSC-SC *Moringa stenopetala* crude extracts of sodium chloride

NMR nuclear magnetic resonance

pH<sub>PZC</sub> pH at point of zero charge

 $pK_{a app}$  apparent  $pK_a$ 

PSD position sensitive detector

PTC purified (or pretreated) Tundulu clays

PXRD powder X-ray diffraction

RTC raw Tundulu clays

TDS total dissolved solids

TO Si tetrahedral sheet and Al octahedral sheet forming a layer in that order

TOT Si tetrahedral sheet, Al octahedral sheet and Si tetrahedral sheet forming a

layer in that order

WWTP wastewater treatment plant

XANES X-ray absorption near edge structure

#### **Appendices**

This thesis is based on studies presented in original publications, which will be referred to by their roman numerals (I-V). Kind permissions were obtained from the publishers. The thesis therefore complements on (not repeat) details of the work which have been published in the scientific articles or in press.

- **I.** Sajidu, S.M.I., Masamba, W.R.L., Henry, E.M.T., Kuyeli, S.M (2007). Water quality assessment in streams and wastewater treatment plants of Blantyre, Malawi. *Journal of Physics and Chemistry of the Earth Parts A/B/C*, 32 (15-18), 1391 1398.
- **II.** Sajidu, S.M.I., Persson, I., Masamba, W.R.L., Henry, E.M.T., Kayambazinthu, D (2006). Removal of Cd<sup>2+</sup>, Cr<sup>3+</sup>, Cu<sup>2+</sup>, Hg<sup>2+</sup>, Pb<sup>2+</sup> and Zn<sup>2+</sup> cations and AsO<sub>4</sub><sup>3-</sup> anions from aqueous solutions by mixed clay from Tundulu in Malawi and characterisation of the clay. *Water SA*, 32 (4), 519-526.
- III. Sajidu, S.M.I., Persson, I., Masamba, W.R.L., Henry, E.M.T (2008). Mechanisms of heavy metal sorption on alkaline clays from Tundulu in Malawi as determined by EXAFS. *Journal of Hazardous Materials*. doi:10.10.1016/j.jhazmat.2008.01.087. (In press)
- **IV.** Sajidu, S.M.I., Henry, E.M.T., Persson, I., Masamba, W.R.L., Kayambazinthu, D (2006). pH dependence of sorption of Cd<sup>2+</sup>, Zn<sup>2+</sup>, Cu<sup>2+</sup>, and Cr<sup>3+</sup>, on crude water and sodium chloride extracts of *Moringa stenopetala* and *Moringa oleifera*. *African Journal of Biotechnology*, 5 (23), 2397-2401.
- V. Sajidu S.M.I., Persson, I., Masamba, W.R.L., Henry, E.M.T (2008). Mechanisms for biosorption of chromium(III), Copper(II) and Mercury(II) on *Moringa oleifera* water extracts. *African Journal of Biotechnology*, 7(6), 800-804.

#### 1. INTRODUCTION

#### 1.1 Overview

#### 1.1.1 Problems of heavy metal pollution

There is widespread recognition that heavy metals can be toxic pollutants and their discharge into surface waters, from natural geochemical and anthropogenic sources, is a global concern (Harrison, 1996). Heavy metals occur naturally in soils and leach into water systems. They are widely used in industry especially in electronics and the rapidly growing information technology sector. Common anthropogenic sources include agricultural activities, atmospheric deposition, road run off, discharges from industrial plants and sewage works, acidic mine effluents and building of reservoirs. Agricultural activities provide important non-point sources of heavy metal pollutants such as cadmium and lead. For example, phosphatic fertilizers are the most ubiquitous source of cadmium contamination because the rock phosphates used for the manufacture of fertilizers have relatively high concentrations of cadmium (Alloway and Ayres, 1995; Harrison 1996; Järup, 2003).

The most common toxic effects of heavy metals result from chronic exposure rather than acute poisoning. Depending on the exposure route of a given heavy metal, its metabolism and storage, chronic exposure may lead to a variety of conditions. For example, chronic intake of high levels of cadmium causes both fibrotic and emphysematous lung damage, and also has major effects in bone and kidney. Itai-itai (ouch-ouch) disease—a syndrome of chronic renal failure and osteoporosis described in the Fuchu area in Japan—is often attributed to high levels of naturally occurring cadmium in the soil (Nishio *et al*, 1999). This was exacerbated by increased industrial exposures around World War II when cadmium was released in significant quantities by mining operations which increased cadmium pollution in surrounding rivers. The cadmium contaminated water was used mainly for rice irrigation, drinking, fishing and washing by people downstream. Chronic exposure to copper can lead to its accumulation in liver, brain, kidney, and cornea, leading to the classic impairment and stigmata of Wilson disease (Roundhill, 2004) and Indian childhood cirrhosis (Tanner, 1998). Lead is known to affect the central nervous system, and may cause retardation in children,

birth defects and possible cancer. Lead interferes with incorporation of iron into the porphyrin precursors of haem; thus, producing anaemia. Patients with lead poisoning have impaired uptake of iodine by the thyroid. It is also antagonistic to calcium because its metabolism parallels that of calcium (Alloway, 1995; Harrison, 1996). Chronic poisoning of inorganic mercury is characterised by neurological and psychological symptoms such as tremor, changes in personality, restlessness, anxiety, sleep disturbance and depression. Methylmercury poisoning results into nervous system damage and intake of high levels can cause death within few weeks. The Minamata catastrophe in Japan in the 1950's was caused by methylmercury carried through contaminated fish (Järup, 2003). The essential trace element zinc plays an important role in cellular metabolism but it also exhibits toxic properties and at high concentrations can affect and impair cellular functions (Rossi *et al*, 1996). Chromium occurs in two redox states, chromium(III) and chromium(VI). The trivalent species occurs at low pH in cationic form and it is less toxic than the hexavalent species which occurs always as an anion. However, the final intracellular product of chromium(VI) is chromium(III) which forms amino acid nucleotide complexes (Roundhill, 2004).

The toxicities of heavy metals are of major concern not only to human beings but also to plants (Hall, 2002) and other living organisms. Lead and zinc have been shown to be the most important toxic heavy metals in captive birds (Aizenberg *et al*, 2006). Although the general population is primarily exposed to heavy metals via food and air, exposure to drinking contaminated waters can also be a major route of heavy metal uptake particularly in developing countries where water sources may be contaminated by incompletely treated industrial or agricultural effluents (Igwe and Abia, 2006).

#### 1.1.2 Heavy metal contamination in Blantyre City streams

This study was motivated due to drastic decline of water quality in terms of heavy metals in streams of Blantyre, the major commercial and industrial city of Malawi. Malawi's economy is heavily dependent on agriculture and poor agricultural practice is a major cause of water resources degradation (DEA, 2002). Although the country is not heavily industrialised, discharge of untreated industrial effluents into surface waters also contributes to water resources degradation especially in urban areas (DEA, 2002). The 2002 State of the Environment Report identified contamination of the water resources arising mainly from

poor sanitation, improper disposal of wastes, agro-chemicals and effluent from industries, hospitals and other institutions as the major threat to water quality (DEA, 2002). Most industries do not have the financial ability to invest in conventional wastewater treatment methods, since such techniques are quite expensive; hence, they tend to discharge their effluents in a non-environment friendly manner.

Specific discharges of heavy metals such as lead, iron and cadmium into the environment particularly in the city of Blantyre have been observed (Lakudzala et al, 1999; Masamba and Chimbalanga, 2001; Matope, 2002; Kadewa et al, 2001). The levels of lead of 0.73 mg/L and 0.096 mg/L have been obtained in Mudi and Limbe rivers of Blantyre, respectively, while the cadmium levels were 0.72 mg/L and 0.86 mg/L respectively (Matope, 2002). Lakudzala et al. (1999) also detected iron levels of up to 1.0 mg/L in Mudi River. These levels are much higher than the acceptable levels of less than 0.05mg/L, and 0.005mg/L for lead and cadmium respectively (WHO, 2004). These unacceptable levels of heavy metals in the Blantyre aquatic environment have been attributed mainly to inadequate treatment of industrial effluents and chemicals from agricultural land runoff (Masamba and Chimbalanga, 2001, Matope, 2002). The problems obtaining in Blantyre are of course typical in many developing countries where costly wastewater treatment processes are unsustainable and therefore use of local materials is the focus. This thesis presents laboratory results on the viability of natural alkaline mixed clays from Tundulu in Phalombe District of Malawi and seed coagulants of Moringa oleifera (locally known as Cham'mwamba) and Moringa stenopetala in removing heavy metals from contaminated water. An understanding of chemical reactions between heavy metals and these materials is essential in designing remediation strategies and managing heavy metal contaminated wastewater.

#### 1.2 Conventional heavy metal removal from water and wastewater

In this section some conventional technologies relating to heavy metal removal from water and wastewater are reviewed. The technologies discussed include, chemical precipitation (involving use of hydroxides, carbonates, or sulphide reagents), solvent extraction, ion exchange, adsorption and sand filtration. The merits and limitations of these methods are discussed.

#### 1.2.1 Chemical precipitation

One of the most common processes of heavy metal removal from industrial wastewater involves chemical precipitation of the metals followed by settling of the metal or filtration. In this process soluble heavy metal salts are converted to insoluble salts which precipitate upon adjustment of the solution pH, addition of a chemical precipitant, and flocculation. Depending on the required cleanup procedures metals can be precipitated as hydroxides, sulphides or carbonates. However, different metal hydroxides have different pH levels for their solubilities; consequently, in a solution mixture of metals such as industrial wastewater at a given pH, some of the metal hydroxides will dissolve and return to the solution as hydroxometal complexes. In that case additional precipitation steps may be required. The precipitation process can also generate colloids that are held in suspension by electrostatic surface charges which cause clouds of counter-ions to form around the particles and give rise to repulsive forces that prevent aggregation, and reduce the effectiveness of solid-liquid separation. Chemical coagulants are therefore used to overcome these forces and increase the particle size through aggregation. Commonly used hydroxide precipitation reagents are magnesium hydroxide, calcium oxide and sodium hydroxide. Sulphide precipitation yields a more complete heavy metal removal than hydroxide precipitation. However, excess sulphides left in the solution are toxic and the resulting sludge is difficult to discharge. This process has therefore limited use compared to hydroxide precipitation. Carbamates obtained as sodium dimethyl dithiocarbamate or sodium diethyldithiocarbamate are also used to precipitate metals in solutions but the process is not effective at acidic pH levels. Depending on reagents used and required system controls this process of heavy metal removal can be costly requiring high capital and operation costs making it very difficult to implement in developing countries (Mier et al, 2001; Chang et al, 2006).

#### 1.2.2 Ion exchange

In ion exchange process, the heavy metal cation is exchanged for a similarly charged ion attached to an immobile solid particle. These particles can either be synthetically produced organic resins or naturally occurring inorganic zeolites. The synthetic organic resins are the predominant type used today because their characteristics can be tailored to specific applications. Ion exchange reactions are stoichiometric and reversible. For example a resin with hydrogen ions available for exchange will exchange those ions for heavy metal ions such as nickel ions from solution in a reaction as follows:

$$2(R-SO_3H) + Ni^{2+} + 2H_2O \implies (R-SO_3)_2Ni + 2H_3O^+$$

where R indicates the organic portion of the resin and  $-SO_3^-$  is the immobile portion of the ion active group. Two resin sites are needed for a divalent ion whereas trivalent ion would require three resin sites. The reactions and processes of heavy metal removal using ion exchange resins have been developed and documented by many authors (Simpson and Laurie, 1999; Elshazly and Konsowa, 2003; Silva and Brunner, 2006; Pehlivan and Altun, 2007). One advantage of the ion exchange process is the ease of separating the solid resin from treated water. However, ion exchanger regeneration process, which is usually done with highly concentrated electrolyte solutions, results in the increase in salt content of the wastewater from the process. Special regeneration chemicals are available but these may be as costly as the continuous use of fresh exchangers (Silva and Brunner, 2006).

#### 1.2.3 Solvent extraction

Solvent extraction involves (i) reaction of an extractant with the metal to form an organometallic complex in the solvent, (ii) stripping whereby the complex is decomposed by addition of sodium hydroxide, ammonia or a weak acid, and (iii) regeneration of the extractant that returns to the extraction section while the metal is transferred to aqueous phase (Roundhill, 2004). Many factors govern the choice of the extractant such as, type of heavy metal being extracted, anions present in the solution that may interfere with organometallic complex formation and also presence of other metals in the solution to be separated. The extractants can be acidic, basic or neutral organic compound with molecular mass of 200 to 450. Examples of acidic extractants include bis (2-ethyl-hexyl)phosphoric acid (DEHPA), alkyl hydroxyoxime (LIX-84) and hydroxyquinoline (KELEX-100). The basic ones include the primary amine (PRIMENE JMT), tertiary amines tri-*n*-octyl amine (Adogen 364, Alamin 366) or the quaternary ammonium salt tri-*n*-alkylmethylammoniumchloride with C6-C8 alkyls (Aliquat 336, Adogen 464) while examples of neutral ones include tri-*n*-butyl phosphate (TBP), tri-*n*-butyl phosphine oxide, and di-hexylsulfide (Černă, 1995). Some advantages of solvent extraction methods are that the process requires low energy and that there is complete regeneration of the extractant. The extracted metal can be obtained in high purity if it is to be reused. However, the strategy is financially driven in terms of costs of the extractants and operating costs.

#### 1.2.4 Adsorption and sand filtration

Ferric salts such as ferric chloride precipitate as amorphous hydrated oxide or oxyhydroxide at neutral to alkaline pH. These precipitates are stable and have reproducible absorptive properties which remain intact although the precipitates transform to crystalline goethite (α-FeOOH) upon aging (Benjamin, 1983). Cationic heavy metal ions such as chromium(III), copper(II), cadmium(II) and lead(II) are absorbed on the ferric hydroxide precipitates at neutral to high pH conditions while heavy metals in anionic compounds such as SeO<sub>4</sub><sup>2-</sup>, CrO<sub>4</sub><sup>2-</sup>, VO<sub>3</sub>(OH)<sup>2-</sup>, AsO<sub>4</sub><sup>3-</sup> absorb at neutral to slightly acidic pH. One problem with this method is that iron replaces heavy metals in complexes of ammonia, chlorides, sulphates cyanides, amines, citric acid, EDTA and many more and therefore the concentrations of such metals may increase in the solutions containing such complexes.

Sand filters have been found to be effective in removing specific heavy metals such as chromium and zinc (Baig *et al*, 2003). The removal efficiency increases with the depth of the sand column. The best results are obtained for a 1.2 m deep column at flow rate of 0.1 m/hr with influent chromium concentration of 250 mg/L (Baig *et al*, 2003). Although sand is readily available the depth requirement entails use of great volumes of sand which consequently create disposal problems after saturation of the sand particles.

#### 1.3 Low-cost methods for heavy metal remediation

#### 1.3.1 Use of natural clay adsorbents

Adsorption of toxic heavy metals by clays is a widely investigated area in the field of pollution control and soil science. The clays are being investigated as alternative natural heavy metal coagulants in order to considerably reduce costs of chemicals compared to the conventional techniques (Bektaş *et al*, 2004). Some of the common clays that have been studied include montmorillonite (Brigatti *et al*, 1995; Auboirox *et al*, 1996), bentonite (Khan *et al*, 1995), vermiculite (Bourlivia *et al*, 2004; da Fonseca *et al*, 2006), illite (Elzinga and Sparks, 2001) and non clay mineral hydroxyapatite (Takeuchi and Arai, 1990; Ma *et al*, 1994; Lower *et al*, 1998; Singh *et al*, 2001; Lusvardi *et al*, 2002).

However incomplete elucidation of mechanisms of the removal of heavy metals by the clays impede their wide spread application. Characteristically clay is the fraction of soil minerals with a maximum size of 2 µm containing structurally two main building blocks of aluminosilicates (Gustafsson *et al*, 2005). There are Si tetrahedra which are composed of one Si atom surrounded by four O atoms and octahedra containing Al or Mg (or sometimes Fe) co-ordinated to six O atoms which may sometimes appear as hydroxyl groups (Figure 1).

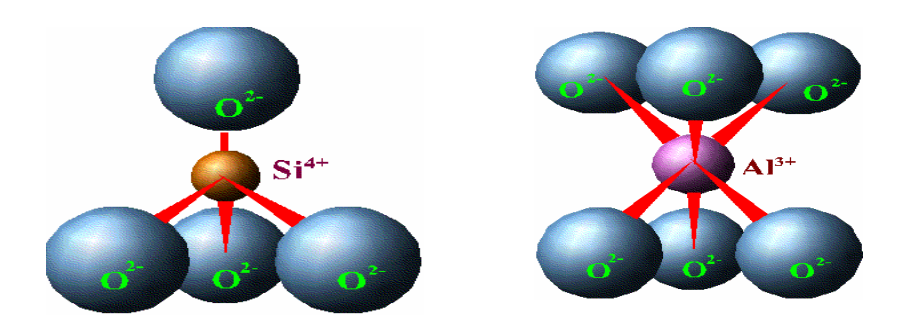


Figure 1: Silicon tetrahedron and aluminium octahedron (Harter, 1998)

The tetrahedra and octahedra are bound together in horizontal two- dimensional arrangements to form sheets and two or three of these sheets are bound vertically to form a layer. The layers are then linked through either cation bridging with fixed cations (mainly  $K^+$ ) or cation bridging with hydrated exchangeable cations or hydrogen bonding. During the formation of the clay minerals, other ions with similar ionic radii may enter the structure to substitute for the central ion that would normally be there. Almost always, the new ion has a lower positive charge; hence, the sheet develops a negative charge proportional to the extent of ion substitution. This phenomenon is called *isormophous substitution*. Geometrically for a cation to fit in the octahedral hole, the ratio of its radius ( $r_c$ ) to that of  $O^{2-}$  ( $r_o$ ) must be between 0.414 and 0.732. The radius ratio ( $r_c/r_o$ ) for cation to fit in the tetrahedral hole must be between 0.225 and 0.414 (Huheey *et al*, 1993). The cations that may fit into the clay's tetrahedral and octahedral holes are presented in Table 1. Aluminium can therefore fit into both the tetrahedral or octahedral hole whereas silicon is always in the tetrahedral hole. Magnesium and iron can substitute aluminium in the octahedral sheet (Gustafsson *et al.*, 2005).

Table 1: Cation: oxygen radius ratio  $(r_c/r_0)$  for various common ions (Gustafsson et al., 2005)

Central ions in tetrahedral hole		Central ions in octahedral hole	
Metal cation	$r_{\rm c}/r_{\rm O}$	Metal cation	$r_{\rm c}/r_{\rm O}$
Si <sup>4+</sup>	0.30	$Al^{3+}$	0.41
Al <sup>3+</sup>	0.41	$Mg^{2+}$	0.58
		Fe <sup>2+</sup>	0.59
		Fe <sup>3+</sup>	0.54
		Zn <sup>2+</sup>	0.42
		Mn <sup>2+</sup>	0.61

Depending on the structure of the layers, the clay minerals are classified as 1:1, 2:1 or 2:1:1. A 1:1 clay mineral has a layer, which is composed of a tetrahedral sheet (*T*) joined to an octahedral sheet (*O*) forming a regular series of *TO TO TO*... A 2:1 mineral has tetrahedral sheet joined to an octahedral sheet which in turn is joined to a tetrahedral sheet forming a regular series of *TOT TOT TOT*... Beside the 2:1 mineral series, a 2:1:1 is composed of an extra octahedral sheet in the interlayer. The schematic packing of the sheets in these minerals is shown in scheme 1 below:

Scheme 1: Schematic packing of sheets in clay minerals

1:1 minerals

		O(Mg/Al/Fe)
0(41)	T(Si)	T(Si)
O(Al) $T(Si)$	O(Al/Mg)	O(Al/Mg)
T(SI)	T(Si)	T(Si)

2:1 minerals

When the octahedral sheet contains divalent ions the mineral is distinguished as trioctahedral clay mineral whereas dioctahedral clay minerals have trivalent ions in the octahedral sheet. Trioctahedral clay minerals can also contain 50% trivalent and 50% monovalent ions in the octahedral sheet. In a dioctahedral clay mineral only  $\frac{2}{3}$  of the octahedral holes are filled with the trivalent ions whereas all the octahedral holes are filled with divalent ions in the trioctahedral clay mineral (Gustafsson *et al*, 2005).

2:1:1 minerals

Smectites, of which montmorillonite is an example, are either trioctahedral 2:1 or dioctahedral 2:1 clay minerals with isormophous substitution in the octahedral or tetrahedral sheet (Gustafsson *et al*, 2005). The general formula for montmorillonite is

$$M^{^{+}}_{x+y}\,(Al_{2\text{-}x}Mg_{x})(Si_{4\text{-}y}Al_{y})O_{10}(OH)_{2}$$

The individual layers therefore have unbalanced negative charge; consequently, monovalent exchangeable cations reside between the layers. These interlayer cations are generally hydrated and readily displaced into solution by other cations, a process called *cation exchange* which is the driving force for the investigation of montmorillonite as a possible heavy metal remover from wastewater. Brigatti *et al* (1995) studied the interaction between montmorillonite and zinc(II) and lead(II) polluted industrial wastewater of different ionic strength ranging from 10<sup>-5</sup> to 1 mol·dm<sup>-3</sup>. The results showed attainment of stationary state of exchange within 20 min indicating a high affinity of zinc(II) and lead(II) for montmorillonite. Zinc(II) was shown to be more easily exchanged than lead(II) due to presence of Zn(II) in the octahedral sites and also formation of Zn(OH)2 sheets or polyhedra in the interlayer similar to brucitic sheets in chlorite. Auboiroux *et al* (1996) studied fixation of zinc(II) and lead(II) by a purified Wyoming Ca-montmorillonite (montmorillonite with calcium(II) exchangeable

cations in the interlayer) at variable ionic strength solutions. Their results indicated stronger lead(II) fixation over zinc(II) at lower ionic strength, contrary to the findings of Brigatti et al. (1995). The difference could be attributed to the different types of montmorillonite in the two cases.

Vermiculites, which are 2:1 sheet silicate minerals, are present in both dioctahedral and trioctahedral forms (Gustafsson *et al*, 2005). However, vermiculites have a higher layer charge than smectites. This means that vermiculites have higher cation exchange capacity (CEC) than smectite. Charge balancing in the interlayer region of vermiculites is made up by hydrated cations such as magnesium(II). Typical trioctahedral vermiculite has the formula:

$$Mg_{0.33}(Mg,Al,Fe^{3+})_{3}(Si_{3}Al)O_{10}(OH)_{2} \\$$

Lead and zinc removals reaching 95% and 96% respectively from solutions containing 100mg/L of the metal had been shown through use of vermiculite adsorbent from Askos area in Greece (Bourlivia *et al*, 2004).

Illite is also a 2:1 clay mineral whose structure is poorly defined. There is some degree of isormophous substitution of Si<sup>4+</sup> for Al<sup>3+</sup> in the tetrahedral silica sheet. The resulting negative charge is balanced by K<sup>+</sup> in the interlayers. The interlayer region may also contain some structural bound water. Sorption of nickel in illite suspension has been studied and has indicated a nickel removal mechanism that involves formation of Ni-Al layered double hydroxides at pH values greater than 6.25 (Elzinga and Sparks, 2001). Takeuchi and Arai (1990) studied the removal of lead(II), copper(II) and cadmium(II) ions from water by the addition of hydroxyapatite (HAP) [Ca<sub>5</sub>(PO<sub>4</sub>)<sub>3</sub>(OH)] and concluded that lead removal was through absorption of lead on the HAP surface followed by cation exchange with calcium. Contrary to this mechanism, Ma (1994) proposed lead immobilisation mechanism by HAP through dissolution of the HAP followed by hydroxypyromorphite [(Pb<sub>10</sub>(PO<sub>4</sub>)<sub>6</sub>(OH)<sub>2</sub>] precipitation on the basis of macroscopic data with direct spectroscopic and diffraction evidence. This mechanism was consistent with later studies (Lower *et al*, 1998; Singh *et al*, 2001; Lusvardi *et al*, 2002). However, the later studies also suggest formation of other solid

lead phases in addition to the hydroxypyromorphite. Although there was significant cadmium(II), copper(II), and zinc(II) removal by HAP no new phases were formed to justify formation of a new stable compound.

In Malawi, deposits of alkaline mixed clays containing some apatite are abundant. In our earlier preliminary work, the alkaline mixed clay samples from Tundulu in Phalombe District, obtained through the Geological Survey of Malawi, indicated high removal of heavy metals such as lead and cadmium (Sajidu *et al*, unpublished).

#### 1.3.2 Uses of Moringa seed powder

Moringa oleifera is a tropical plant belonging to the family of Moringaceae. It is native to sub-Himalayan North-western India, Arabia and Pakistan (Williamson, 1975; Anonymous, 1993). The plant was distributed to some areas of tropical Asia in prehistoric times and to other parts of the world during the British colonial era. It is now widely cultivated and occurs naturalised and semi-wild in Africa, Asia, Central America, Caribbean Islands and South America. The tree is extremely fast growing with a three months old tree reaching 8 feet. It is adaptable to a wide range of soils and environments and survives in semi-arid conditions of tropical and subtropical regions (Anonymous, 1993). The synonym of M. oleifera Lam is Moringa pterygosperma Gaertn and vernacular names include Chamwamba or Kangaluni (Malawi), Drumstick tree, West Indian Ben, Idaga Manoye (Yoruba) and Ben Tree (India) (Williamson, 1975; Morton, 1991). The M. oleifera is the most widely distributed, well-known and studied species of the family Moringaceae because of its previous economic importance as a source of the commercially important 'Ben oil' and more recently, as a multipurpose tree for arid lands and a source of water purifying agents for developing countries. The wide range uses of Moringa include food (Morton, 1991; Makkar and Becker, 1996; Lalas and Tsaknis, 2002; Richter et al, 2003; Soliva et al, 2005), medicine (Sofowora, 1993; Leuck and Kunz, 1998; Guevara et al, 1999; Tahiliani and Kar, 1999; Gupta et al, 1999; Ghasi et al, 2000; Karadi et al, 2006), fodder and as a living fence (Pratt et al, 2002). The roots are used as a horseradish substitute and the young green pods are a delicacy in India while the leaves are edible and good sources of Vitamin A and C, and protein concentrate (Price, 2000). The tree appears in the pharmacopoeia of Africa, Asia, South America and the Caribbean for the traditional treatment of many illnesses including asthma, diarrhoea, fever, cough, stomach pains, blood pressure, heart problems, epilepsy and joint diseases; consequently, several bio-active constituents have been identified. The dried pods and husks are used in production of activated carbon (Pollard *et al*, 1995; Warhust *et al*, 1997a; Warhust *et al*, 1997b; Warhust *et al*, 1997c)

Moringa stenopetala, which is commonly known as the African Moringa, is native to Ethiopia and Northern Kenya. M. stenopetala produces larger seeds and leaves than M. oleifera and it is more drought tolerant but slightly less cold tolerant (Jahn, 1991). Figure 2 shows seed husks and kernels of M. oleifera and stenopetala.



Figure 2: Seeds of *M. oleifera* and *M. stenopetala* 

*M. oleifera* is one of the natural coagulants that have been extensively studied in clarification of turbid water. Jahn (1981) first confirmed the coagulating properties of *Moringa* seeds after observing women in Sudan use the seeds to clarify the turbid Nile water at home. Studies on

the efficiency of *M. oleifera* seed extract as a water coagulant had been carried out by several workers (Muyibi, 1994; Muyibi *et al*, 2002; Muyibi and Alfugara, 2003; Ndabigengesere *et al*, 1995; Ndabigengesere *et al*, 1998; Sutherland *et al*, 1994). Muyibi (1994) reported that the seeds also reduce alkalinity and have buffering capacity in high alkaline waters. In Malawi water treatment trials using *M. oleifera* were done at Thyolo Water Treatment Works (Sutherland *et al*, 1994). The plant consisted of up flow contact clarifiers followed by rapid gravity filters. Inlet water turbidity (270 to 380 NTU) were reduced consistently to below 4 NTU using a dosage of 75 mg/l of seed extract. This reduction was comparable to that of alum (50 mg/l). The *M. oleifera* seed extracts have also been shown to reduce faecal coliform counts in contaminated water (Henry *et al*, 2004). With initial coliform count of about 350 in 100 mL of turbid water, a dose of 120 mg of *M. oleifera* seed powder reduced the coliform count to about 53 (about 85% reduction).

The mechanism for the reaction of coagulation by *M. oleifera* has been partially elucidated by several workers. The coagulating property of the seeds has been attributed to water-soluble cationic polypeptides with molecular weights ranging from 6000 to 16000 Daltons (Ndabingesere *et al*, 1995; Gassenschimdt *et al*, 1995; Jahn, 1988). The amino acids present in the coagulating proteins of *M. oleifera* seeds are glutamine, arginine and proline (Gassenschmidt *et al*, 1995). Okuda *et al* (2001) have also reported that *Moringa* contains another active coagulant, a non-protein organic compound with a coagulation mechanism involving enmeshment by a net-like structure.

Very little work is reported on the use of *M. stenopetala* for water purification in literature. It is observed that crushed powder of 1 to 1½ seeds can be used to clean 1 litre of muddy water, and also microorganisms settling out with the solids (Deutsch – Äthiopischer, 2000).

Although use of *Moringa* seeds in water turbidity and microorganism reduction is well documented, limited studies have been carried out to determine the ability of the seeds to remove heavy metal cations from water and wastewater (Mataka *et al*, 2006; Kumari *et al*, 2006; Sharma *et al*, 2007).

#### 2. GENERAL AND SPECIFIC OBJECTIVES

The general objective of the study was to investigate the potential of natural coagulants (alkaline clays and *Moringa* seed extracts) in heavy metal removal from contaminated water and understand mechanisms of the removal in order to stimulate the development of locally available solutions for heavy metal water pollution abatement in Malawi. Prior to the main activities, a quick survey of heavy metal levels and other physicochemical parameters in various streams and wastewater treatment plants in the City of Blantyre (Paper I) was carried out.

#### The specific objectives were:

- a. To determine acid base characteristics of Tundulu mixed alkaline clays and their mineralogical composition and investigate the potential of the clays in removing heavy metals from water (Paper II).
- b. To examine the potential of water and sodium chloride extracts of *Moringa seeds* in removing heavy metals from water (Paper IV).
- c. To explore mechanisms through which heavy metals are sorbed onto the mixed alkaline clays, and extracts of *Moringa* seeds using extended x-ray absorption fine structure (EXAFS) (Papers III and V).

The thesis is organised as follows. The first chapter has presented a brief introduction to general problems associated with heavy metals. Recent published work done in Blantyre City related to heavy metal contamination is summarised. A review of conventional methods for heavy metal removal from contaminated water is described. The last sections of the chapter describe the chemical structures of clays and their use for heavy metal removal. A brief review on the use of *Moringa* for water clarification has been presented.

Chapter 3 describes materials and methods. In this chapter methods used for determination of metal cations (Pb, Cd, Zn, Cr, Fe, Cu, Ni, Na and K) and anionic parameters (PO<sub>4</sub><sup>3-</sup>, NO<sub>3</sub>-, SO<sub>4</sub><sup>2-</sup>) including biochemical oxygen demand have been described. The chapter also describe how the clays were purified by removing carbonates, iron oxides and organic matter. Potentiometric titrations of the clays, mineralogical analysis using powder x-ray diffraction (PXRD) and heavy metal adsorption properties of the clays are then discussed in detail with sections devoted to theories of the methods. Use of extended x-ray absorption fine structure in identifying chemical environments around heavy metals sorbed onto the clays is described. The last sections of the chapter describe how water and sodium chloride soluble extracts of *Moringa* seeds were prepared and used for heavy metal removal from contaminated water including use of EXAFS in order to understand the metal sorption reactions by *Moringa*.

Presentation of the results and discussion for the water and wastewater quality analysis in Blantyre City is made in chapter 4. This is followed by characterisation of the clays and their metal sorption properties. Results for the sorption of heavy metals by water and sodium chloride extracts of *Moringa* seeds are presented. Mechanisms through which heavy metals are sorbed onto the clays and Moringa as obtained by EXAFS are discussed. The practical applications, limitations of the work, areas for future study and highlights of this thesis are presented in chapter 5.

#### 3. METHODOLOGY

This section of the thesis gives details (not normally included in the scientific articles) of methods used in the work.

#### 3.1 Physicochemical quality of water and wastewater in Blantyre

#### 3.1.1 Water sampling methods and study sites

Water quality describes the biological, chemical and physical characteristics of the water (Anonymous, 1996). Each of these aspects have their standards developed by national and international water authorities defining the limits within which water can be considered safe for a particular use. Biological components refer to the number and types of organisms in the water. Physical attributes such as temperature and turbidity may indicate presence of certain effluents in the area. Chemical parameters include pH, alkalinity, hardness, nitrates, nitrites, ammonia, phosphates, biochemical oxygen demand (BOD) and metals (including heavy metals). Techniques of water sampling for determination of water quality parameters are dependent on the parameters to be analysed. There are two methods for water/wastewater sampling in streams. One is grab sampling where all the test material is collected at one time. The results of analyses are therefore only applicable at the time the sample is collected. The second method is composite sampling which consists of numerous individual discrete samples taken at regular intervals over a period of time. The results in this case represent the average quality of the water during the collection period. In this thesis grab sampling technique was adopted.

Figure 3 is a map of the study sites. These included the three major streams in Blantyre City passing through industrial areas namely Nasolo (Figure 4), Mudi and Limbe. Wastewater at Limbe (Figure 5) and Soche wastewater treatment plants (WWTP) were sampled at stations before and after treatment. Sampling was done in February 2005 using grab sampling. Samples were collected using one-litre plastic bottles that had been cleaned by detergents, soaked in 10% nitric acid and rinsed several times with distilled water. Storage and treatment of the water samples were done according to APHA (1985). Six one-litre samples were

collected at each point three of which were acidified using 1 mL of concentrated nitric acid for metal analyses in order to minimize precipitation and adsorption on the walls of the container.

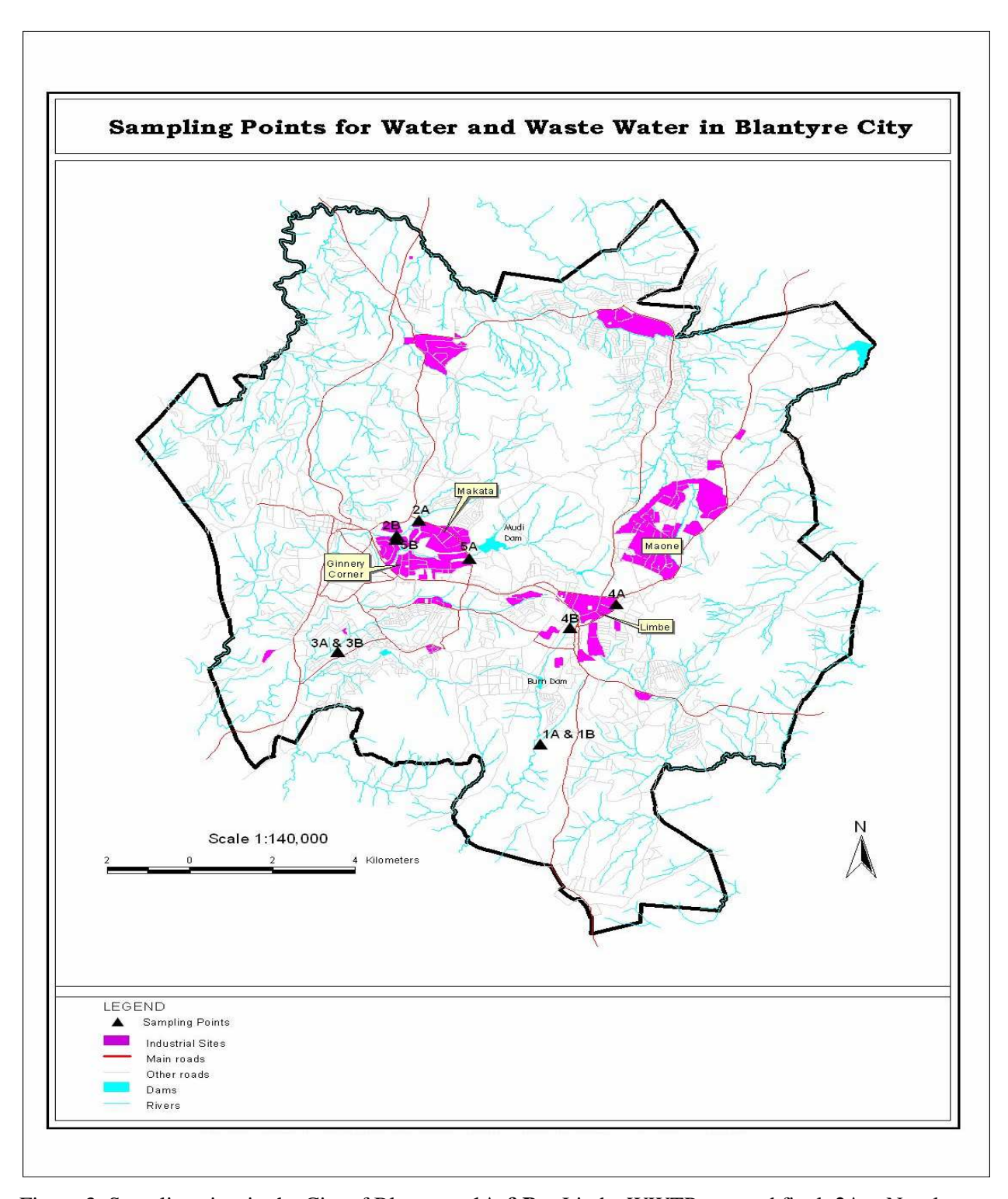


Figure 3: Sampling sites in the City of Blantyre: **1A &B** = Limbe WWTP raw and final, **2A** = Nasolo River near Grace Bandawe, **2B** = Nasolo River at SR Nicolas, **3A&B** = Soche WWTP raw and final, **4A** = Limbe stream at Mpingwe Sports Club, **4B** = Limbe Stream at Kara Mansion, **5A** = Mudi River near MDI. **5B** = Mudi River at SR Nicolas



8.9.2005

Figure 4: Photo of water sampling at one of the sample points (Nasolo river). The dirty dark water was due to a suspected broken sewer line from industrial area emptying the effluent into the stream.

Figure 5: Photo of part of Limbe Wastewater Treatment Plant. The plant uses a pond system.

# 3.1.2 Brief theory of analytical methods for determination of nitrates, phosphates, sulphates and biochemical oxygen demand

Molecular absorption spectroscopy is commonly used for determination of molecular species such as phosphates and nitrates in water. When a molecule is excited by ultraviolet and visible radiation ( $\lambda = 190 - 1000$  nm) an electron is promoted from low energy molecular or atomic orbital to higher energy orbital. The energy, hv, of the photon is exactly the same as the energy difference between the two orbital energies and this is characteristic of the given molecule or atom (Scoog *et al*, 2004). In the case of a coloured molecule the intensity of the absorbed photons (the absorbance, A) is proportional to the concentration of the molecules in a sample as described by the Beer – Lambert law:

(i) 
$$A = \mathcal{E}bc$$

where  $\varepsilon$  is a wavelength-dependant molar absorptivity coefficient with units of mol<sup>-1</sup>·dm<sup>3</sup>cm<sup>-1</sup>, b the path length and c the concentration of the analyte in the sample. Usually experimental measurements are made in terms of transmittance, T, defined as:

(ii) 
$$T = \frac{I}{I_o}$$

where I is the radiation intensity after it passes through the sample and I<sub>o</sub> is the initial light intensity. The relation between A and T is:

(iii) 
$$A = -\log T$$

An unknown concentration of an analyte can be determined by measuring the amount of radiation that the sample absorbs and applying the Beer- Lambert law. If the absorptivity coefficient is not known, the unknown concentration can be determined using a calibration curve of absorbance versus concentrations derived from standards.

In calorimetric determination of phosphate in water samples, ammonium molybdate reacts with orthophosphate in an acid medium to form phosphomolybdate complex which can be reduced to yield an intense blue colour suitable for calorimetric measurement. The phosphomolybdate complex is either molybdenum blue or molybdenum yellow which when reduced further results in molybdenum yellow. Molybdenum blue is a sensitive large 13–molecule complex with phosphate as its central molecule. It radiates a blue colour often due to the reduction of some of the molybdenum atoms in the complex from a +6 oxidation state to a +5 or some other oxidation state in between. The absorbance of the complex (A<sub>470</sub> nm) is proportional to the concentration of the compound (and also the concentration of phosphate that has reacted from the water sample). The chemical reactions for the formation of the complex are (Omae *et al*, 2006):

(iv) 
$$PO_4^{3-} + 12(NH_4)_2 MoO_4 + 24H^+ \rightarrow (NH_4)_3 PO_4.12 MoO_3 + 21NH_4^+ + 12H_2O_4 + 12H_4O_4 + 12H_4O$$

(v)  $(NH_4)_3 PO_4.12MoO_3 + (reducing agent) \rightarrow (molybdenum blue) + (weaker reducing agent)$ 

The reducing agent could be stannous chloride, ascorbic acid or vanadomolybdophosphoric acid. Stannous chloride and ascorbic acid form molybdenum blue which is directly related to phosphate concentration in a sample, while vanadomolybdophosphoric acid forms molybdenum yellow which is reduced to molybdenum blue.

In the determination of sulphate by turbidimetric method, barium ions react with sulphate ions to produce a milky (cloudy) precipitate of barium sulphate:

(vi) 
$$Ba^{2+} + SO_4^{2-} \rightarrow BaSO_4$$

The milky appearance of the barium sulphate, turbidity, is proportional to the concentration of sulphate in the sample. The absorbance of the turbidity  $(A_{420})$  is measured using a spectrophotometer and concentration of the sulphate is calculated using a regression based on external standards (APHA, 1985). It is important that factors such as time and rate of stirring and time of standing of the precipitate before measurement be as uniform as possible for accurate and reproducible results. Since the particle size of a precipitate depends on the relative supersaturation, R, of the system (Scoog *et al*, 2004), where

$$R = \frac{Q - S}{S}$$

where Q is the concentration of the solute at any instant and S, the equilibrium solubility such that the particle size of the precipitate varies inversely with the average relative supersaturation during the time when the reagent is being introduced. The barium sulphate precipitate can thus be made more colloidal than crystalline by, for example using concentrated solution (i.e adding excess BaCl<sub>2</sub>), adding the BaCl<sub>2</sub> quickly and slow stirring of the solution, factors that will increase the relative supersaturation and reduce the particle size of the crystals (APHA, 1985).

Several methods for determination of nitrates exist. One of the most used methods is the salicylate colorimetric method (Yang *et al*, 1998; Monteiro *et al*, 2003) which involves heating the sample under acidic conditions (sulphuric acid) to convert the nitrate ions (NO<sub>3</sub><sup>-</sup>) to nitronium ions (NO<sub>2</sub><sup>+</sup>) which react with salicylate under alkaline conditions (sodium hydroxide) to form a yellow nitrobenzoic compound. The reaction occurs in two steps:

(vii) 
$$2H_2SO_4 + NO_3^- \longrightarrow 2HSO_4^- + NO_2^+ + H_2O$$

(viii) 
$$HOC_6H_4COO^- + NO_2^+ \longrightarrow NO_2C_6H_4COO^- + HO^-$$

The intensity of the colour of the nitrobenzoic compound, determined at  $\lambda = 220$  nm or 410 nm, is proportional to the concentration of nitrates in the sample.

BOD<sub>5</sub> is a measure of the amount of organic matter in water samples. It is indirectly determined by measuring the amount of oxygen consumed by microorganisms in biodegrading organic constituents of the water. This is therefore done by measuring concentration of oxygen (by the Winkler Method) in the sample before and after incubating the water sample for 5 days at 20°C (APHA, 1985). The initial step in the determination of the dissolved oxygen involves oxidation of manganese(II) to manganese(III) in alkaline solution.

(ix) 
$$8OH^{-}(aq) + 4Mn^{2+}(aq) + O_{2}(aq) + \longrightarrow 2H_{2}O(1)$$
  $4Mn(OH)_{3}(s)$ 

Subsequently, sodium or potassium iodide is added to the solution which is oxidised by the manganese(III) hydroxide in acidic environment.

(x) 
$$2Mn(OH)_3(s) + 3\Gamma(aq) + \longrightarrow 6H^+(aq)$$
  $I_3^-(aq) + 3H_2O(l) + 2Mn^{2+}(aq)$ 

The formed triiodide  $(I_3^-)$  is titrated with sodium thiosulphate.

(xi) 
$$2S_2O_3^{2-}(aq) + I_3^{-} \longrightarrow (aq)$$
  $S_4O_6^{2-}(aq) + 3I^{-}(aq)$ 

1 mole of dissolved oxygen is therefore stoichiometrically equivalent to 4 moles of thiosulphate used in the final titration reaction. It is important to make sure that oxygen is neither introduced nor lost from the sample during the reaction stages.

#### 3.1.2.1 Determination of phosphates

The water samples were digested using perchloric acid. An aliquot of the water sample (50.0 mL) was acidified to methyl orange (pH = 2 - 3) with concentrated nitiric acid and then about 5 mL of concentrated nitric acid was added. The resultant sample mixture was then evaporated on a hot plate till the volume reduced to about 15 mL after which, it was cooled and mixed with concentrated nitric acid (5 mL). 70% perchloric acid (10 mL) and a few boiling chips were added. The mixture was heated gently until dense white fumes of perchloric acid appeared. A drop of phenophthalene solution was added to the digested solution and neutralised with dropwise addition of 6 mol·dm<sup>3</sup> sodium hydroxide till solution turned pink at the end point. The solution was then filtered and made up to 100 mL mark with distilled water. Exactly 50.0 mL of the filtered solution was then decolorised using 0.2 g of activated charcoal. Then 20 mL of vanadomolybdate reagent was added into 25.0 mL of the decolourised sample and made up to 100 mL mark. The absorbance of the sample at a wavelength of 470 nm was read using a JENWAY 6405 UV/Vis spectrophotometer. The vanadomolybdate reagent had been prepared by dissolving 25g of ammonium molybdate in 400 mL of distilled water (solution A) and 1.25 g of meta vanadate in 300 ml of boiling water to which 250 mL of concentrated nitric acid were added (solution B). Solutions A and B were then mixed in 1 L volumetric flask and made up to the mark with distilled water (APHA, 1985).

Phosphate standard stock solution was prepared by dissolving 439.3 mg of anhydrous  $KH_2PO_4$  (dried for 1 h in an oven at  $105^{\circ}C$ ) in deionised water and making up to 1000 mL mark (303.6 mg/L  $PO_4^{3-}$ ).

#### 3.1.2.2 Determination of nitrates

The water samples were filtered and 20.0 ml of each filtered sample was mixed with 10 mL of 0.5% sodium salicylate in 250 mL volumetric Erlenmeyer flask and evaporated to dryness. After cooling, 1mL of concentrated sulphuric acid was added to the residues and left to stand

for 10 minutes. Then 25 mL of deionised water was added and warmed gently to dissolve any residues. Finally 10 mL of sodium hydroxide (25% w/v) was added and the mixture (yellow in colour) was quantitatively transferred into a 100 mL volumetric flask and then diluted to the mark with deionised water. Absorbance of the solution mixtures were then measured at wavelength of 410 nm with a JENWAY 6405 UV/Vis spectrophotometer. Stock solution of nitrate (443 mg/L NO<sub>3</sub><sup>-</sup>) was prepared by dissolving anhydrous potassium nitrate (predried in oven at 105°C for 24 h) in a 1-Litre volumetric flask and making up to the mark (Yang *et al*, 1998).

#### 3.1.2.3 Determination of sulphates

20 mL of buffer solution, comprising of a mixture of 30 mg MgCl<sub>2</sub>.6H<sub>2</sub>O, 5 g sodium acetate and 20 mL glacial acid, was mixed with 100 mL of sample in an Erlenmeyer flask while stirring. A spoonful (teaspoon size) of BaCl<sub>2</sub> crystals was added to the mixture while stirring. The stirring continued for 1 minute and then the solution was poured into absorption cell and the absorbance was measured at 420 nm using a JENWAY 6405 UV/Vis spectrophotometer. 1000 mg/L of sulphate stock solution was prepared by dissolving 1.479 g of anhydrous Na<sub>2</sub>SO<sub>4</sub> in distilled water and making up to 1000 mL mark (APHA, 1985).

#### 3.1.2.4 pH determination

pH values of the water samples were recorded at Soche WWTP immediately after sample collection using a Kent Eil 7020 pH meter. Soche WWTP is within a radius of less than 8 km from the other sampling points.

#### 3.1.2.5 Determination of total dissolved solids (TDS)

A measured volume of the sample was mixed thoroughly by stirring with a magnetic stirrer and filtered using glass fibre filters. The filtered sample was evaporated to dryness in a tared beaker. The mass gained was equal to TDS of the sample per initial volume.

#### 3.1.2.6 Determination of BOD<sub>5</sub>

BOD<sub>5</sub> was measured at Soche WWTP using the Winkler Method as described in APHA (1985). Dilution water was prepared by adding 5 mL each of FeCl<sub>3</sub>. 6H<sub>2</sub>O (0.125g in 1 Litre

of deionised water), anhydrous CaCl<sub>2</sub> (6.875g in 250 mL of deionised water), MgSO<sub>4</sub>. 7H<sub>2</sub>O (6.25g in 250mL of deionised water) and phosphate buffer of pH 7.2 to 5 litres of deionised water. The sample (20.00 mL) was placed in a sample flask to which distilled water was added and 2.0mL each of phosphate buffer, magnesium sulphate, calcium chloride and ferric chloride solutions for each litre of dilution water. After diluting and mixing well and allowing no air in the sample, it was then pipetted into two BOD bottles, one for incubation for 5 days at 20<sup>o</sup>C and the other one for the determination of initial dissolved Oxygen. During the determination of dissolved oxygen levels, a stopper was carefully removed from a reagent bottle containing a sample and 2 mL of MnSO<sub>4</sub>, H<sub>2</sub>O solution (182g in 500 mL of deionised water) was added. Then, 2 mL of alkali-azide-sodium iodide solution (5g NaN<sub>3</sub>, 250g NaOH and 70g NaI in 500 mL of deionised water) was pipetted into the reagent bottle by lowering the tip of the pipette below the surface of the sample. The stopper was then replaced onto the bottle and inverting the bottle at least 5 times to mix the contents. After allowing the developed precipitate to settle, 2 mL of conc. sulphuric acid was added to the mixture in the reagent bottle. The stopper was then replaced and the reagent bottle shaken until all the precipitate dissolved. A sample aliquot (15.00 mL) was pipetted into a 250 mL Erlenmeyer flask before titrating with standardized 0.025 mol·dm<sup>-3</sup> sodium thiosulphate solution. The difference in the amount of dissolved oxygen in the 5 day - incubated sample and the non-incubated one was used to calculate the BOD<sub>5</sub> value.

### 3.1.3 Theoretical description of analysis of metal ions by atomic absorption spectroscopy

Metal levels in water samples are commonly determined using atomic absorption spectroscopy (AAS). The technique involves measuring the amount of radiant energy absorbed by the sample. An atom of an element has its own distinct pattern of wavelengths at which it will absorb energy because of its unique electron configuration (Scoog *et al*, 2004). This uniqueness allows for the qualitative and quantitative analysis of the pure atom. During the determination, the water sample is atomized in a flame followed by absorption of radiation from a radiation source by the free atoms which undergo electronic transitions from the ground state to excited electronic states. A detector measures the intensity of the radiation and when some of the radiation is absorbed by the atoms, the radiation intensity is reduced. It

is this reduction that is measured as absorption or absorbance. During the atomisation step the sample solution is dispersed into a fine spray of the metal atom particles in the flame. The particles are subsequently vapourized into neutral atoms, ionic species and molecular species; hence, it is important to set the instrument parameters such that the radiation from the source, typically a hollow cathode lamp (HCL), is directed through the region of the flame that contains the maximum number of neutral atoms. The radiation produced by the HCL is emitted from excited atoms of the same element which is being determined. Therefore, the source energy corresponds directly to the wavelength which is absorbed by the atomized sample. This method provides both sensitivity and selectivity since other elements in the sample will not generally absorb the chosen wavelength. To reduce background interference, the wavelength of interest is isolated by a monochromator placed between the sample and the detector. A schematic diagram of the AAS instrumental set up is shown in Figure 6. Molecular absorption bands in the sample and also absorption by the flame gases may overlap with the desired atomic absorption line resulting in artificially high absorption and improper high calculations for the solution metal concentration. The total measured absorbance, A<sub>T,</sub> is the sum of the analyte absorbance, A<sub>A,</sub> plus the background absorbance, A<sub>B</sub> (Scoog *et al*, 2004):

$$A_T = A_A + A_B$$

The scheme that attempts to measure  $A_B$  in addition to  $A_T$  and obtain the true analyte absorbance by subtraction ( $A_A = A_T - A_B$ ) is called background correction. Three methods are typically used for background correction. Continuum source background correction uses a deuterium lamp and the analyte hollow cathode lamp (HCL) which are directed through the atomizer at different times. The HCL obtains  $A_T$  while the deuterium lamp estimates  $A_B$ .  $A_A$  is obtained by calculating the difference between the two using processing electronics or computer systems. In Zeeman effect background correction, magnetic field is used to degenerate spectral lines into components with different polarization characteristics.  $A_A$  and  $A_B$  can be separated because of their different magnetic and polarization behaviours. In Smith-Hieftje background correction the HCL is pulsed with first a low current and then a

high current. The low-current mode obtains  $A_T$  while  $A_B$  is estimated during the high-current pulse (Scoog *et al*, 2004).

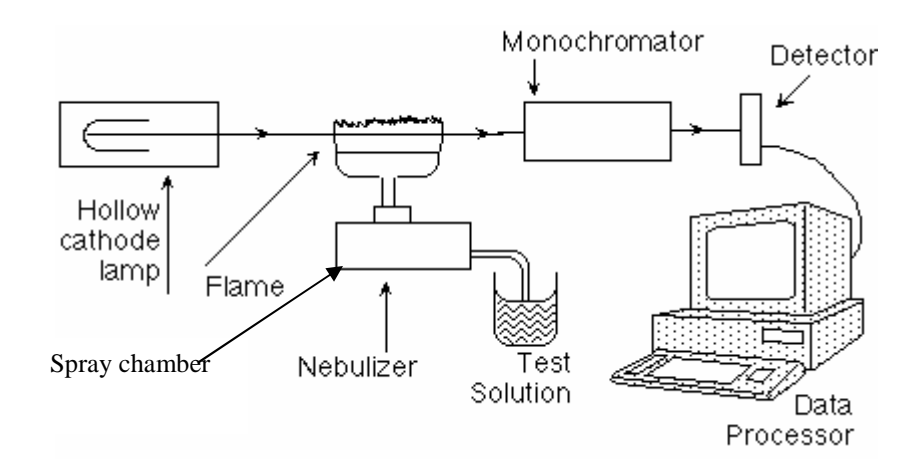


Figure 6: Schematic diagram of atomic absorption spectroscopy experimental set up.

The absorbance is proportional to the concentration of the absorbing atoms in the sample as stated by Beer's law (Skoog *et al*, 2004). However, applying the Beer's law directly in atomic absorption spectroscopy is difficult due to variations in the atomization efficiency from sample matrix and nonuniformity of concentrations and path length of analyte atoms. Concentration measurements are usually determined from a working curve after calibrating the instrument with standards of known concentrations.

#### 3.1.3.1 Sample digestion prior to metal ion determination

Water samples for the determination of metals were prepared by the conventional nitric acid digestion (APHA, 1985). A well-mixed sample (100.0 mL) was transferred to a 250ml flask and 5ml of concentrated nitric acid was added to it. The mixture was then brought to a slow boiling and evaporated on a hot plate until the volume was reduced to about 20 mL. About 5 mL of concentrated nitric acid was added to the solution and the flask covered with a watch glass before heating it to obtain a gentle refluxing. The heating continued whilst adding 5 mL portion of nitric acid until the solution became light coloured clear solution. Finally 1-2ml of nitric acid was added to dissolve any remaining residues and later the solution was quantitatively filtered into 100ml volumetric flask and diluted to the mark.

#### 3.1.3.2 Determination of metal ions

The concentrations of metal ions in water and wastewater samples were determined using Atomic absorption spectrophotometer (Shimadzu AA – 680/GV-S) at Chancellor College (University of Malawi). The metal ions determined were sodium and potassium (common alkali metals), and chromium, manganese, iron, copper, zinc, cadmium and lead (heavy metals). During the removal studies, concentrations of chromium, copper, zinc and cadmium were also determined using an atomic absorption spectrophotometer (Perkin Elmer AAnalyst 100) while mercury, lead and arsenic were determined using an Inductively Coupled Plasma Emission Spectrometer at the Department of Soil Sciences (SLU).

#### 3.1.4 Sources of clay samples and brief description of purification procedures

Clays used for heavy metal removal work in this study were collected from the Geological Survey of Malawi but originally from Tundulu hills in the Phalombe District. Adsorption experiments were done using both purified and raw clays. The purified clays are called 'Purified Tundulu clays (PTC) while the raw clays are called 'Raw Tundulu Clays (RTC). The clay purification procedure was done as described in literature (Kunze and Dixon, 1986; Ammann, 2003) and summarized below.

Purifications or pre-treatments of clays are designed to remove as many impurities as possible and the selected methods must have minimum effect on the actual constituents of the clays (Kunze and Dixon, 1986; Ammann, 2003). Generally, three categories of impurities are identified; carbonates, iron oxides and organic matter. Removal of these impurities is desirable in order to obtain definitive x-ray diffraction and differential thermal analysis patterns, infrared spectra and other mineralogical analytical results. Carbonates, particularly poorly crystalline carbonates, cause a great deal of scatter resulting in poor x-ray diffraction patterns. Such carbonates also increase the complexity of differential thermal analysis patterns. Their presence in clay also reduces the efficiency of hydrogen peroxide during the removal of organic matter. Removal of carbonates is achieved by reacting the clay with a weak acid such as sodium acetate-acetic acid buffer or dihyrogen ethylenediaminetetraacetate till there is no more evolution of carbon dioxide. Organic matter has cementing effect on the

clays and therefore its removal is necessary for analysis of dispersed clays. Hydrogen peroxide is used to oxidize organic matter and its maximum efficiency requires acidic medium. It is therefore necessary to remove carbonates prior to organic matter removal. Clays containing free iron oxides are difficult to disperse. Mineral separation is difficult when the clay particles are coated with iron oxides. Furthermore, the iron oxides fluorescence when a copper induced x-ray radiation is used for diffraction analysis giving an increased background count and a general decrease in quality of the diffraction pattern. Removal of iron oxides involves reduction of iron(III) to dissolved free iron(II). The sodium dithionate-citrate procedure is one of the recommended procedures with minimum destructive action to the clay. In this method (Kunze and Dixon, 1986) sodium citrate is used to chelate both iron(II) and iron(III) in the clay. Sodium bicarbonate buffers the solution to prevent precipitation while sodium dithionate reduces the iron. After removal of carbonates, iron oxides and organic matter the clay sized particles (less than 0.002 mm) are separated from sand and silt by different methods such as sedimentation. In the sedimentation procedure the particles are homogeneously dispersed in water and allowed to stand undisturbed as the particles sediment. Particles of diameter, D, settle below distance, h, from bottom of the container at time, t, according to Stokes' law:

(i) 
$$D = K \left(\frac{h}{t}\right)^{1/2}$$

where  $K = \left[\frac{18\eta}{(\rho - \rho_o)g}\right]^{1/2}$  and  $\eta = \text{the liquid viscosity}, \rho = \text{the particle density}, \rho_o =$ 

the liquid density

#### 3.1.4.1 Removal of carbonates

Raw clay (100 g) was dispersed in 100 mL of 1 mol·dm<sup>-3</sup> sodium acetate-acetic acid buffer (8.2 g sodium acetate and 6 g pure acetic acid per 100 mL of water, pH = 4.8). The mixture was stirred from time to time for a few days until there was no more evolution of carbon dioxide bubbles (which indicate presence of carbonates). The slurry was then centrifuged in readiness for removal of iron oxides.

#### 3.1.4.2 Removal of iron oxides

The centrifuged clay was dispersed in 270 mL citrate buffer (115 g (0.37 mole) sodium citrate dihydrate, 8.5 g (0.1 mole) sodium hydrogencarbonate and 70 g (1.2 mole) sodium chloride per litre). pH was adjusted to 8.3 and 20 g of sodium dithionate was added. The slurry was stirred for 70 h, centrifuged and washed four times with a solution of 0.5 mol·dm<sup>-3</sup> sodium chloride and 0.025 mol·dm<sup>-3</sup> hydrochloric acid. The whole procedure was repeated once more.

#### 3.1.4.3 Removal of organic matter

500 mL of 0.1 mol·dm<sup>-3</sup> sodium acetate solution and 170 mL of 30% w/w aqueous hydrogen peroxide solution were added to the slurry (after removal of iron oxides) and the mixture was stirred for 10 h at 90 °C and then for 20 h at room temperature. The clay was then washed three times with 1 mol·dm<sup>-3</sup> sodium chloride solution. Finally the clay was washed with distilled water to remove excess salt, dried at room temperature and then ground to powder in readiness for fractionation.

#### 3.1.4.4 Fractionation of the clay

The dried clay was transferred to a cylinder (5 cm in diameter and 30 cm high) and diluted to a height of about 25 cm with deionised water. The suspension was shaken to homogeneity and allowed to stand undisturbed for 8 h. The clay suspension above 10 cm was siphoned to a bucket and concentrated by centrifugation.

## 3.1.5 Brief theory of qualitative mineralogical analysis using Powder X-Ray Diffraction (PXRD)

Crystalline solids have their own characteristic x-ray powder patterns which may be used as a 'finger print' for their identification (Brindley and Brown, 1980). X-rays are produced by a beam of electrons of sufficient kinetic energy generated by a heated tungsten filament that is accelerated through 30 to 40 kV. This high voltage rapidly draws the electrons to a metal target of copper fixed to the anode which they strike with very high velocity. They ionize some of the copper 1s electrons. An outer orbital electron (2p or 3s) immediately drops to

occupy the vacant 1s position and the energy released in such a transition appears as x-ray radiation. For copper the 2p to 1s transition is known as  $K_{\alpha}$  and has a wavelength of 1.5418Å.  $K_{\beta}$  refers to the 3p to 1s transition with wavelength of 1.3922 Å.  $K_{\alpha}$  is more intense than  $K_{\beta}$ and in diffraction experiments where monochromatic radiation is required it is desired that the other wavelengths are filtered out. In this case a nickel filter, which absorbs  $K_{\beta}$  to a large extent but not  $K_{\alpha}$ , is used. A monochromator can also be used to discriminate the other wavelengths. The three major components in a diffraction experiment are the x-ray source, sample and the detector for recording the diffracted x-rays. In powder x-ray diffraction (PXRD) a monochromatic beam of x-rays strikes a finely powdered sample of ideally randomly orientated crystallites. The powder form makes it certain that all the possible orientations of lattice planes are available. The path difference between reflected beams at successive planes at a glancing angle of  $\theta$  is easily seen from Figure 7 to be  $2d \sin \theta$ , d being the spacing of the planes. The actual orientation of the planes is defined by the Miller indices hkl. Miller indices represent an atomic plane in a crystal lattice. They are defined as the reciprocals of the fractional intercepts which the plane makes with crystallographic axes. In order to label a plane of atoms in a cubic crystal system, for example, firstly the intercepts of the plane on the x-, y- and z- axes are identified. Then the reciprocals of the points of intersection are taken and written in parenthesis as (hkl) where h = 1/a, k = 1/b and l = 1/cand a, b, and c are the corresponding distances along the x-, y- and z- axes respectively. An example of a (210) plane is shown in Figure 8. Unit cells are characteristic of crystalline solids. For example, in cubic crystals distance, d, between adjacent crystal planes is given by

$$d = \frac{a}{\sqrt{h^2 + k^2 + l^2}}$$

If a diffracted beam is formed when a beam of x-rays passes through a crystal, it must be in such a direction that it may be considered as derived by reflection of the incident beam from one of the sets of lattice planes, but a reflection can only occur if the Bragg's law (given below) is satisfied,

(i) 
$$n\lambda = 2d \sin \theta$$

where  $\lambda$  is the wavelength of the x-rays being used. Rewriting the Bragg's law gives:

(ii) 
$$\sin \theta = n \lambda 2d$$

showing that the possible  $2\theta$  values which can give reflections are determined by the unit cell dimensions contained in the d value.

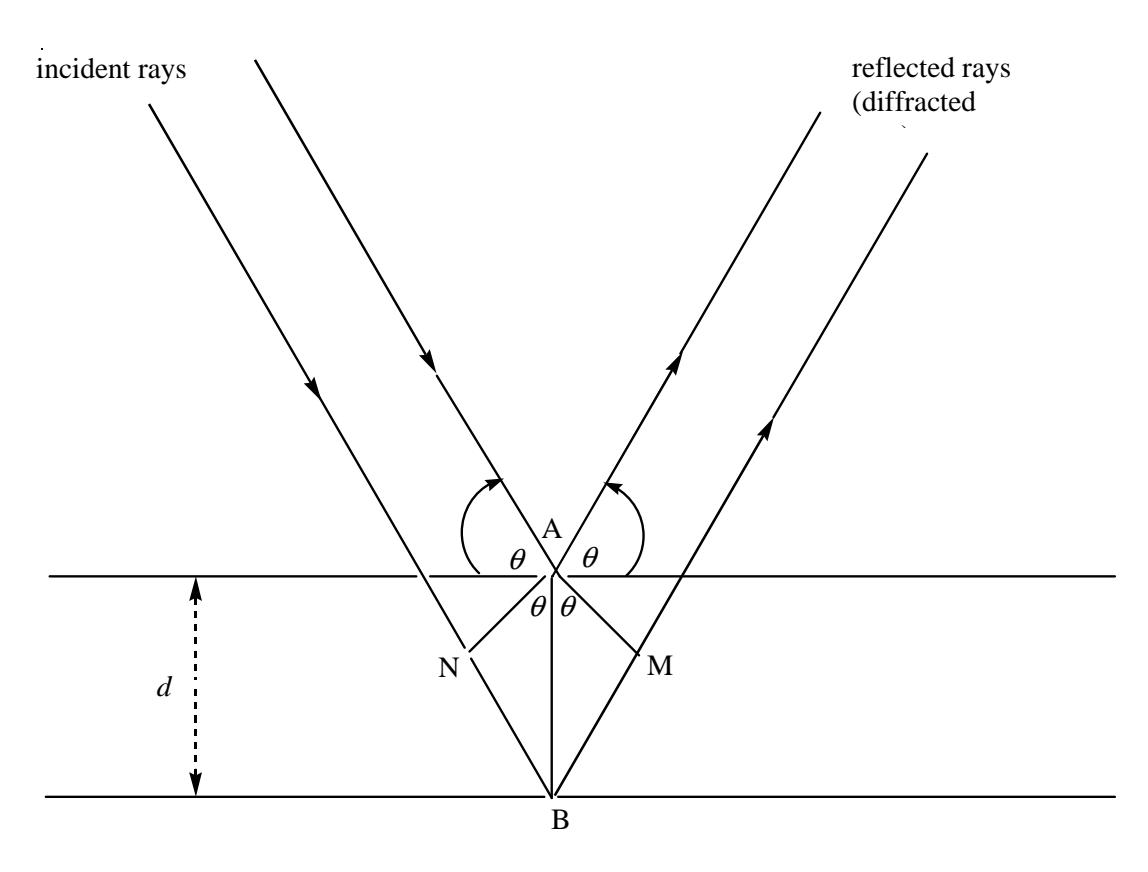


Figure 7: Path difference between reflections from successive planes. The path difference =  $NB + BM = 2d \sin \theta$ 

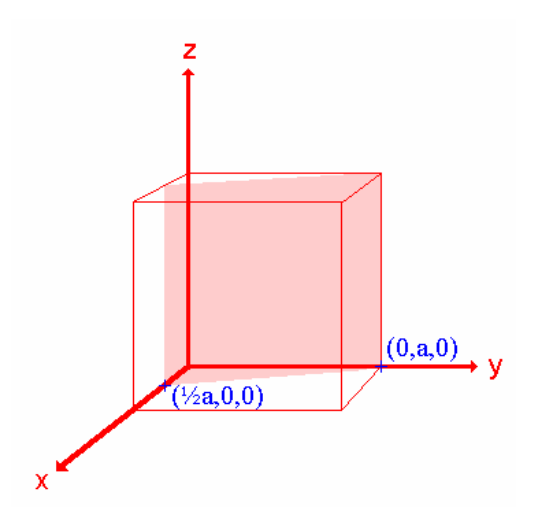


Figure 8: A (210) Miller plane. The intercepts on x-, y- and z- axes are at  $\frac{1}{2}$ a, a and  $\infty$ , respectively. Fractional intercepts are  $\frac{1}{2}$ , 1,  $\infty$ . Reciprocals of the fractional intercepts are 2,1,0; hence, the Miller indices are (210)

Different methods are used for observing diffracted rays. A movable detector such as a Geiger counter connected to a chart recorder (diffractometer) can be used or the sample can be surrounded with a strip of photographic film (Debye Scherrer method) or a position sensitive detector (PSD) can be used (Cullity, 1978). A typical PXRD spectrum (Figure 9) is a plot of diffracted intensities against the detector angle  $2\theta$ . Interplanar spacing, d, that corresponds to the h, k, l parameters in the Miller planes that caused the reflection can be calculated since

(iii) 
$$d = \lambda/2\sin\theta$$

The d spacing and the corresponding Miller indices h, k, l, are used to calculate the dimensions of the unit cell.

Phase identification is therefore done by searching crystal database for compounds with the same or similar unit cells. One of the most common uses of PXRD is phase identification (search/match) in samples containing multiphasic mixture of compounds. The procedure involves comparing the measured pattern against the International Centre for Diffraction Data/Joint Committee on Powder Diffraction Standards (ICDD/JCPDS) powder file data

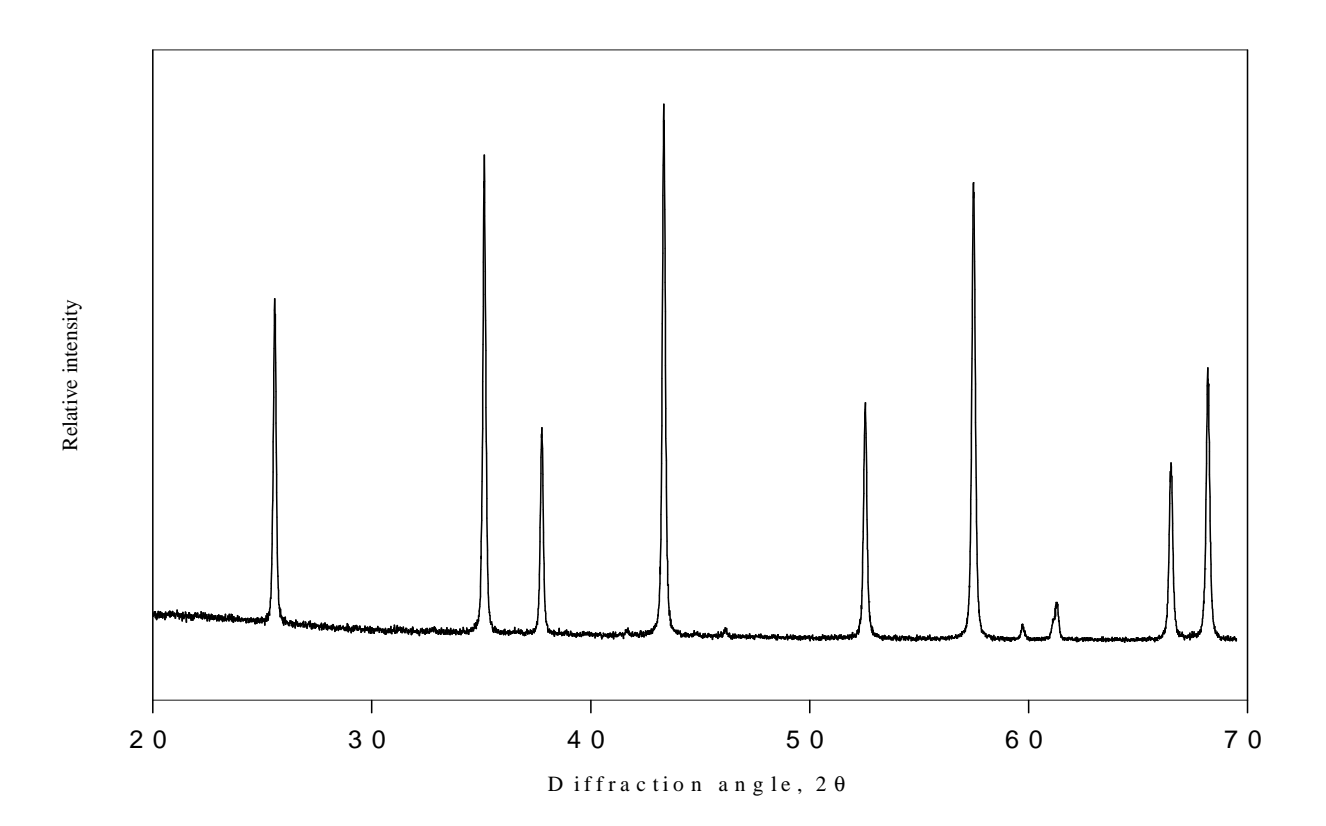


Figure 9: An example of a PXRD plot. This is a PXRD pattern of well crystallized  $\alpha$ -Al<sub>2</sub>O<sub>3</sub>.

base or mineralogical data base such as Mineralogy Database (2006). These contain powder patterns for a very large number of compounds.

Search/match identification of the PXRD plot is done as follows: (i) d spacing of the three most intense reflections are located in decreasing order at  $2\theta$  angles of 43.5°, 35.0° and 58.0°. (ii) the corresponding d values are calculated using the Bragg's law. The results of the two steps are shown in Table 2.

Table 2: Identification of the three most intense reflections in a PXRD plot (Figure 9) and calculation of the corresponding d values

Intensity order	1	2	3
2θ(°)	43.5	35.0	58.0
θ(°)	21.75	17.5	29.0
$d$ (Å) (= $\lambda/2\sin\theta$ )	2.08	2.56	1.59

 $<sup>\</sup>lambda = 1.5418 \text{ Å for the Cu K}_{\alpha}$ 

The d values (and the corresponding relative intensities of the reflections) are then compared with available values in database. For example, crystallographic data for corundum ( $\alpha$ -Al<sub>2</sub>O<sub>3</sub>) obtained from Mineralogy Database (2006) are presented in Table 3. The x-ray diffraction data (last row) matches well with the results of Figure 10; hence, the compound with this plot is identified as corundum. The best match to the d spacing is normally in agreement of  $\pm 0.01$  Å. If a sample is pure, then every reflection recorded matches well with the ones in database. Identification of multiphasic mixture can be difficult as the three strongest lines in the plot may not all come from the same phase. As such an examination of different combinations of strong reflections is done until a phase is identified. Then reflections from that phase are ignored and the process of matching the remaining reflections is done.

Table 3: A section of crystallographic data for corundum obtained from the Mineralogy Database (2006)

Corundum Crystallography	
Axial Ratios	a:c = 1:2.72995
Cell Dimensions	a = 4.751, c = 12.97, Z = 6; V = 253.54 Den(Calc) = 4.01
Crystal System	<u>Trigonal – Hexagonal Scalenohedral</u> H-M symbol (3 2/m)
	Space Group: R 3c
X Ray Diffraction	By intensity(I/Io): 2.085(1), 2.552(0.9), 1.601(0.8),

#### 3.1.5.1 Powder X-ray diffraction of the clay samples

In this study room temperature XRD patterns for the RTC and PTC were collected in transmission mode using a PW1710 diffractometer (at the department of Forest Soils, SLU) with monochromatic  $CuK_{\alpha l}$  and  $CuK_{\alpha l}$  ( $\lambda_l$ =1.54060Å and  $\lambda_l$ = 1.54439 Å) radiation that was selected using a 0.01 mm Ni-filter. X-rays which were produced at the x-ray source (copper radiation) were passed through the 0.01 Ni-filter for homogenizing the x-ray radiation giving pure  $CuK_{\alpha}$  radiation which was diffracted by the sample. The data were collected in the range from 2.0 to  $60.0^{\circ}$  (20) by a linear PSD which was set at a step size of  $0.020^{\circ}$  (20) and counting time of 1.0 s per step. The diffractometer was operated by computer software from Phillips called automatic powder diffraction (APD).

Identification of minerals in the clay from the XRD patterns was performed 'by hand' using search-match JCPDS-files published by the Joint Committee on Powder Diffraction Standards (JCPDS, 1974) together with diffraction profiles obtained from standards of clay minerals as reported in literature (Mineralogy Database, 2006; Brindley and Brown, 1980). The final plot of the powder pattern was created using Microsoft Excel software on raw data text files.

#### 3.1.6 Theoretical summary of cation exchange capacity for clays

Cation exchange capacity (CEC) of clay is the degree to which it can exchange and adsorb cations. Most clay particles have negative charges on their surfaces resulting from isomorphic substitution in the tetrahedral and octahedral sheets of the clay mineral. Cations may adsorb to the negative charges and the resulting CEC is independent of pH. Cations may also be adsorbed to dissociated aluminol groups on the edges of the clay minerals. The CEC resulting from adsorption on aluminol or silanol clay mineral edge groups is pH dependent because the actual dissociation of the silanol and aluminol groups depends on pH. Most methods of CEC determination are based on saturating the sample with one cation, washing the excess and finally replacing the cation with another cation and then analytically determining the amount of the replaced cation. Barium(II) (Rhoades, 1982), cationic surfactants (Janek and Lagaly, 2003) and metal organic complexes (Pleysier and Cremers, 1975; Chhabra et al, 1975; Bergaya and Vayer, 1997; Meir and Kahr, 1999) are some of the cations used for CEC determination. The affinity of clays for metal organic complexes is very high and the exchange reaction is achieved in one single treatment step. In this work cation exchange capacity of both purified and raw clays was determined using copper bisethylenediamine (Bergaya and Vayer, 1997) as described below.

#### 3.1.6.1 Preparation of 0.5 M copper bisethylenediamine

26.89 g CuCl<sub>2</sub> (0.2 mole) was dissolved in 200 mL distilled water. 30.05 g ethylenediamine (33.39 ml, 0.5 mole) was dissolved in 500 mL distilled water. The complex was formed by adding 50 mL of the CuCl<sub>2</sub> solution to 102 mL of the ethylenediamine solution. The addition

of slight excess amine ensures complete complex formation. The solution was then diluted with distilled water to 1 L to give  $0.05 \text{ mol} \cdot \text{dm}^{-3} \left[ Cu(EDA)_2 \right]^{2+}$ .

#### 3.1.6.2 CEC determination

0.3 to 0.4 g (exact mass of each sample was recorded) of dry clay was weighed in a centrifuge tube. 4.0 mL of the complex solution was diluted to 25 mL with distilled water and added to the clay. The samples were shaken for 30 min and then centrifuged. The experiment was done on three samples on each of the PTC and RTC for statistical interpretation. The concentration of copper(II) in the supernatant was then determined by atomic absorption spectroscopy. The concentration of copper(II) adsorbed was calculated as the difference between the total copper(II) added and the concentration of copper(II) remaining in the supernatant. CEC was then calculated as twice the amount of copper(II) adsorbed per gram of dry clay given as cmol<sub>c</sub> per dry gram of the dry clay. The clay was dried at 105 °C overnight for the CEC calculation.

#### 3.1.7 Brief theory of acid-base properties of the clay

Potentiometric acid-base titration is used to study amphoteric properties of many materials such as oxides, oxide-type and clay minerals. The data can be used to show how charge of the mineral surface varies with pH. The data can also be used to calculate the total amount of acid base active sites and the microscopic acidity constants  $pK_{a_1app}$  and the pH of charge balance (point of zero charge, pH<sub>PZC</sub>) (Stumm, 1992).

In theory (Stumm, 1992) a clay mineral surface, after contact with water, contains  $\equiv SOH$  groups, where  $\equiv S$  represents the surface while OH is the attached hydroxyl group. These groups can dissociate or be protonated in the same way as water and form  $\equiv SO^-$  and  $\equiv SOH_2^+$  surface sites, respectively. The total concentration of acid base active sites is expressed by:

(i) 
$$\{ \equiv SOH_{tot} \} = \{ \equiv SOH_2^+ \} + \{ \equiv SOH \} + \{ \equiv SO^- \}$$

The curl brackets, { }, are used to denote concentration of species on surface of clays whereas the square brackets, [ ], denote concentration of species in solution.

 $\equiv SOH_2^+$  is thus regarded as a diprotic acid with the following two dissociation steps:

(ii) 
$$\equiv SOH_{2}^{+} \implies \equiv SOH_{+} H_{+}^{+} \qquad K_{a_{1}app}^{S} = \frac{\left\{ \equiv SOH_{2}^{+} \middle| H_{+}^{+} \right\}}{\left\{ \equiv SOH_{2}^{+} \middle| H_{2}^{+} \right\}}$$

and

(iii) 
$$\equiv SOH \implies \equiv SO^{-} + H^{+} \qquad K^{S}_{a_{2}app} = \frac{\left\{ \equiv SO^{-} \right\} \left[ H^{+} \right]}{\left\{ \equiv SOH \right\}}$$

The total concentration of surface charge  $\{Q\}$  is the difference between positive and negative surface sites:

(iv) 
$$\{Q\} = \{ \equiv SOH_2^+ \} - \{ \equiv SO^- \}$$

The mean number of protons bound per surface site:

(v) 
$$Z = \frac{\{ \equiv SOH_{2}^{+} \} - \{ \equiv SO^{-} \}}{\{ \equiv SOH_{tot} \}} = \frac{\{Q\}}{\{ \equiv SOH_{tot} \}}$$

which has a domain of -1 to +1. Titration with acid therefore increases Z from 0 to +1.  $\{Q\}$  at given point in the potentiometric titration process is calculated by subtracting the total concentration of  $H^+$  in the solution (not absorbed) from the added  $H^+$ .

(vi) 
$$C_A - C_B - [H^+] + [OH^-] = \{ \equiv SOH_2^+ \} - \{ \equiv SO^- \} = \{ Q \}$$

where  $C_A$  and  $C_B$  are added amounts of acid and base per litre of the mineral suspension respectively.

A major significant difference between acids in homogenous aqueous solution and on surfaces is that the acidity constant in aqueous solution has one value independent of conditions, while the acidity constants of surface sites vary with the surface charge, thus with pH in the aqueous phase. When the net charge of the surface is positive (Z > 0),  $\equiv SOH_2^+$  will, due to repulsive electrostatic forces, dissociate easier than on a surface with no net charge (Z = 0), and the easiness to dissociate increases with increasing positive charge. In the same way, the acidity constant decreases with increasing negative net surface charge. Thus, as Z is a function of pH,  $K_a^s$  also varies with pH.

At each titration point  $K_{\text{a app}}^{\text{S}}$  can be calculated using equation (ii). When pH is less than  $pH_{\text{PZC}}$  equation (ii) can be simplified by assuming that  $\equiv SO^-$  is negligible and then

(vi) 
$$\{\equiv SOH_{tot}\} \approx \{\equiv SOH_2^+\} + \{\equiv SOH\} \text{ and } \{Q\} \approx \{\equiv SOH_2^+\} \text{ while }$$

$$Z = \frac{\left\{ \equiv SOH_2^+ \right\}}{\left\{ \equiv SOH_{tot} \right\}}$$

This implies that

(vii) 
$$K^{S}_{a_{I}app} = \frac{(\{\equiv SOH_{tot}\} - \{Q\}).[H^{+}]}{\{Q\}}$$

Similarly  $K_{a2}^s$  which is determined by the base titration of the mineral suspension is calculated as follows

(viii) 
$$K^{s}_{a_{2}app} = \frac{\{Q\}[H^{+}]}{\{\equiv SOH\} - \{Q\}}$$

At high pH such as during titration of the suspension with a base uptake of carbon dioxide from the atmosphere can lead to formation of carbonate giving erroneous results. Therefore the base titration has to be performed in carbon dioxide free conditions. The intrinsic acidity constant,  $K_{a \text{ int } r.}^{s}$  for the surface, which is a constant valid for uncharged surface, can be obtained by linear extrapolation of the  $\log K_a^s$  versus Q to the Q = 0 point since

(ix) 
$$\log K_a^{\rm S} = \log K_{\rm a intr}^{\rm S} - mQ$$

where m is a coefficient.

When 
$$\left\{ \equiv SOH_2^+ \right\} = \left\{ \equiv SO^- \right\}$$

(x) 
$$pH_{PZC} = \frac{1}{2}[pK_{a_1,intr} + pK_{a_2,intr}]$$

In a salt type mineral or a sample containing many minerals the points of zero charge depend not only on the pH but also on activities of all the other potential determining ions and such a point of zero charge corresponds to the pH of charge balance of potential determining ions (Stumm, 1992).

#### 3.1.7.1 Potentiometric titrations

Suspensions of 6.0 g sample per litre (both for the PTC and RTC) were prepared. 50 mL of the clay suspension was titrated with 0.0213 mol·dm<sup>-3</sup> nitric acid stepwise from 0 to 20 mL at increments of 0.1 mL using Metrohm 665 Dosimat titrator. The pH reading after equilibration of each step was recorded using Ross Sure Flow combination electrode Orion 8172 suitable for pH determination in suspensions. During the titration the flask containing the suspension was covered with parafilm to avoid formation of carbonates at pH greater than 6. A similar titration on a new suspension was done with 0.020 mol·dm<sup>-3</sup> NaOH. The volume,  $V_e$ , corresponding to total proton monolayer coverage (which in turn was used to calculate  $\{\equiv SOH_{tot}\}$ ) was calculated from the pH versus  $V_t$  (volume of acid added) plot. The concentration,  $\{Q\}$ , at every titration point and the mean number of protons per surface site (Z) were also calculated.

Tables 4 and 5 show how  $pK_{a_1}$  and  $pK_{a_2}$  at each titration point were calculated respectively from the acid and base titrations of the clay suspensions.

Table 4: Calculation of p $K_{a_1 \text{ app}}$  from acid titration of the clay suspension

a	b	С	d	e	f	g	h	i	j
$V_{ m ad}$	$pH_{eq}$	$[H^{+}]$	$V_{\rm tot}$ (50	{≡SOH <sub>tot</sub> }	$C_{\mathrm{A}}$	Q	Z	$K_{a_1^{app}}$	$pK_{a_1app}$
		10 <sup>-b</sup>	+ a)	((50*5.398.1	(0.0213*a/d)	(f-c)	(g/e}	(e-g)*c/g	(-log(i))
				$0^{-4})/d)$					

 $V_{\rm ad}$  = volume of acid added to the 50 mL clay suspension; pH<sub>eq</sub> = the equilibrium pH of the suspension measured after the addition; [H<sup>+</sup>] = concentration of H<sup>+</sup> calculated from equilibrium pH;  $\{\equiv SOH_{\rm tot}\}$ = concentration of acid-base sites at a given titration point and 5.398.10<sup>-4</sup> mol·dm<sup>-3</sup> is the total acid-base sites calculated from equilibrium volume;  $C_{\rm A}$  = the total acid concentration added; Q = total concentration of surface charge; Z = mean number of protons bound per surface site;  $K_{\rm a_1 app}$  = apparent first acidity constant; p $K_{\rm a_1 app}$  = apparent p $K_{\rm a_1}$ .

Table 5: Calculation of p $K_{a, app}$  from base titration of the clay suspension

a	b	С	d	e	f	g	h	i	j	k	1
$V_{ m ad}$	$pH_{eq}$	$[H^+]$	pOH <sub>eq</sub>	[OH]	$V_{ m tot}$	{≡SOH <sub>tot</sub> }	$C_{\mathrm{B}}$	Q	Z	$K_{a_2}$	$K_{a_2}$
		10 <sup>-b</sup>	(14-b)	10 <sup>-d</sup>	(50	((50*5.39	(0.02*a/f	(h-	(i/g)	app	app
					+ a)	$8.10^{-4})/d)$	)	e)		(i*c/(	(-
										g-i))	log(k
											))

 $V_{\rm ad}$  = volume of base added to the 50 mL clay suspension; pH<sub>eq</sub> = the equilibrium pH of the suspension measured after the addition; [H<sup>+</sup>] = concentration of H<sup>+</sup> calculated from equilibrium pH; pOH<sub>eq</sub> = the equilibrium pOH after addition of the base; [OH] = concentration of OH from equilibrium pOH; { $\equiv SOH_{\rm tot}$ }= concentration of acid-base sites at a given titration point and 5.398.10<sup>-4</sup> mol·dm<sup>-3</sup> is the total acid-base sites calculated from equilibrium volume;  $C_{\rm B}$  = the total base concentration added; Q = total concentration of surface charge; Z = mean number of protons bound per surface site;  $K_{\rm a_2app}$  = apparent second acidity constant; p $K_{\rm a_2app}$  = apparent p $K_{\rm a_2}$ .

#### 3.1.8 Background information on adsorption of heavy metal cations on clays

Removal of metal cations and anions by clay minerals is controlled by parameters such as charge characteristics of the clay. Charge characteristics include the magnitude of the active sites as determined in potentiometric titrations and cation exchange capacity which has two

components; namely, the permanent negative charge generated by isormophous substitution within the octahedral and tetrahedral sheets of the silicate layers and pH dependent charge arising from dissociation of edge hydroxyl groups. The pH dependent charge may also be contributed by dissociation of other acid groups present such as humic acids particularly in unpurified clay minerals (Adhikari and Singh, 2003; Serrano et al, 2005). In addition to the clay charge properties, metal uptake is also influenced by the characteristic of the metal ion itself such as its ionic radius, charge size and soft – hard acid – base properties (McBride, 1994). Many researchers have investigated the influence of other factors on metal uptake by clays and soils in general such as metal concentrations (Coles and Yong, 2002), presence of competing ions (Auboiroux et al, 1996; Breen et al 1999), pH (Maguire et al, 1981; Barrow et al, 1981; Barbier et al, 2000; Coles and Yong, 2002; Echeverria et al, 2005), temperature (Adhikari and Singh, 2003; Bektas et al, 2004) and ionic strength (Auboiroux et al, 1996; Breen et al 1999; Echeverria et al, 2005). Of all these factors, pH is considered as the 'master variable' controlling ion exchange, dissolution/precipitation, reduction/oxidation, adsorption, hydrolysis and complexation reactions (McBride, 1994). For each adsorbent and metal ion there is a narrow pH interval of about 2 pH units within which uptake of the given metal ion increases from nearly zero to almost 100 percent. The pH decreases the positive charge or increases the negative charge on the adsorbing material, modifies the metal speciation, displaces surface complexation reaction equilibria and also controls the direction of metal cation/proton competition reactions for the negative sites on the adsorbent (Stumm, 1992). The metal cation can be up-taken either by cation exchange or by specific chemical sorption. Absorption into the clay adsorbent structure and precipitation on the surface are also possible irreversible uptake mechanisms (Harter, 1983). These metal sorption mechanisms may occur at different solution pHs for different metals with a possibility of a combination of them at some pH ranges. Metal surface adsorption is characteristic of an inner sphere complex formation. An inner sphere complex can be distinguished from an outer sphere complex by dependence of the metal sorption on ionic strength. Strong dependence on ionic strength indicates formation of outer sphere while non-dependence on ionic strength is characteristic of inner sphere complex formation (Stumm, 1992; Lutzenkirchen, 1997). pH<sub>PZC</sub> values can also be used to distinguish inner and outer sphere complex formation. 100 percent metal sorption occurring below adsorbent's pH<sub>PZC</sub> value is typical of inner sphere complex while

adsorption metal uptake occurring above  $pH_{PZC}$  is characteristic of outer sphere complex. The opposite is true for anion uptake.

While most metal uptake studies by clay minerals have used single clay minerals, this study investigated the dependence of heavy metal uptake on pH by alkaline mixed clay minerals (PTC and RTC) which were qualitatively characterized by PXRD as described above (section 3.1.5.1). The heavy metal cations investigated were chromium(III), copper(II), zinc(II), cadmium(II), mercury(II) and lead(II) cations and the arsenate anion. The studies were performed by batch equilibrium experiments in the pH range 3.0 to 9.0.

#### 3.1.8.1 Preparation of metal solutions

An 0.50 mmol·dm<sup>-3</sup> (103.6 mg/L) aqueous stock solution of lead(II) was prepared by dissolving anhydrous Pb(NO<sub>3</sub>)<sub>2</sub>, analytical grade reagent, declared impurity of less than 0.5% (BDH) in deionized water. An 0.6 mmol·dm<sup>-3</sup> (67.44 mg/L) aqueous stock solution cadmium(II) was prepared by dissolving Cd(NO<sub>3</sub>)<sub>2</sub>·4H<sub>2</sub>O analytical grade reagent, declared impurity of less than 1% (BDH) in deionized water. A 1.25 mmol·dm<sup>-3</sup> (78.44 mg/L) aqueous stock solution of copper(II) was prepared by dissolving Cu(NO<sub>3</sub>)<sub>2</sub>·H<sub>2</sub>O analytical grade reagent, declared impurity of less than 0.2% (Mallinckrodt Chemical Works) in deionized water. A 1.25 mmol·dm<sup>-3</sup> (81.74 mg/L) aqueous stock solution of zinc(II) was prepared by dissolving Zn(NO<sub>3</sub>)<sub>2</sub>·6H<sub>2</sub>O analytical grade reagent, declared impurity of less than 0.2% (Mallinckrodt Chemical Works) in deionized water. A 1.00 mmol·dm<sup>-3</sup> (74.92 mg/L) aqueous stock solution of arsenate was prepared by dissolving Na<sub>2</sub>HASO<sub>4</sub>·7H<sub>2</sub>O declared impurity of less than 0.5% (MERCK) in deionized water. A 2.10 mmol·dm<sup>-3</sup> (109.2 mg/L) aqueous stock solution of chromium(III) was prepared by dilution of a 1.4 mol·dm<sup>-3</sup> Cr(ClO<sub>4</sub>)<sub>3.6</sub>H<sub>2</sub>O stock solution (prepared from chromium(III) perchlorate hexahydrate, Cr(ClO<sub>4</sub>)<sub>3</sub>·6H<sub>2</sub>O in 1.0 mol·dm<sup>-3</sup> hydrochloric acid). An 0.50 mmol·dm<sup>-3</sup> (100.3 mg/L) aqueous mercury(II) trifluoromethanesulfonate solution was prepared by dissolving anhydrous Hg(CF<sub>3</sub>SO<sub>3</sub>)<sub>2</sub> in deionized water at pH 2.0 adjusted by addition of nitric acid. pH values of the solutions are shown in Table 6. Theoretical calculations performed from computer program Visual MINTEQ, Version 2.32 (Gustafsson, 2005) at the solutions' pH values indicate that most of the metal species in solution are free metal cations (Table 6).

Hg(CF<sub>3</sub>SO<sub>3</sub>)<sub>2</sub> and Cr(ClO<sub>4</sub>)<sub>3</sub>·6H<sub>2</sub>O are not available in the program for the theoretical speciation calculations.

Table 6: metal speciation in stock solution as calculated by Visual MINTEQ program

Reagent	Solution	Solution	Species	Species concentration
	concentration	pН		(mmol·dm <sup>-3</sup> )
	(mmol·dm <sup>-3</sup> )			
Pb(NO <sub>3</sub> ) <sub>2</sub>	0.50	5.43	Pb <sup>2+</sup>	0.491
			PbNO <sub>3</sub> <sup>+</sup>	0.006
			PbOH <sup>+</sup>	0.002
Cd(NO <sub>3</sub> ) <sub>2</sub> .4H <sub>2</sub> O	0.60	5.76	Cd <sup>2+</sup>	0.598
			CdNO <sub>3</sub> <sup>+</sup>	0.002
Cu(NO <sub>3</sub> ) <sub>2</sub> .H <sub>2</sub> O	1.25	5.33	Cu <sup>2+</sup>	1.235
			CuNO <sub>3</sub> <sup>+</sup>	0.008
			CuOH <sup>+</sup>	0.005
			Cu <sub>2</sub> (OH) <sub>2</sub> <sup>2+</sup>	0.001
$Zn(NO_3)_2.6H_2O$	1.25	5.31	$Zn^{2+}$	1.244
			ZnNO <sub>3</sub> <sup>+</sup>	0.006
Na <sub>2</sub> HASO <sub>4</sub> .7H <sub>2</sub> O		8.17	HAsO <sub>4</sub> <sup>2-</sup>	0.946
			H <sub>2</sub> AsO <sub>4</sub>	0.054

#### 3.1.8.2 Metal adsorption

7.5 mL of 0.1 mol·dm<sup>-3</sup> NaNO<sub>3</sub> was pipetted into each of 12 centrifuge tubes. 2.5 mL of clay suspension (either PTC or RTC prepared as explained in Section 3.1.7.1) and 0.5 mL of a given metal solution from its stock concentration were added to the centrifuge tube. Appropriate amount of acid (20 mmol·dm<sup>-3</sup> HNO<sub>3</sub>) or base (20 mmol·dm<sup>-3</sup> NaOH) was added to adjust pH to a certain value. The mixture was shaken for 48 h and then centrifuged for 15 min at 3000 rpm using KUBOTA KS-5200C centrifuge. 3-4 mL of the supernatant was taken, acidified with a drop of concentrated nitric acid and analyzed for the given metal concentration on an atomic absorption spectrophotometer (Perkin Elmer AAnalyst 100) in the case of cadmium(II), chromium(III), copper(II) and zinc(II). Lead(II), mercury(II) and arsenic(V) determination in the supernatant was done using an Inductively Coupled Plasma

Emission Spectrometer. The pH in the remaining supernatant in the centrifuge tubes was recorded as the equilibrium solution pH. Percentage metal uptake (%E) was calculated by use of equation (i)

(i) 
$$\%E = \frac{(C_o - C)x100}{C_o}$$

where  $C_o$  and C are the initial and final concentrations respectively of the metal ions in solution.

### 3.1.9 Heavy metal uptake mechanism using Extended X-Ray Absorption Fine Structure (EXAFS) spectroscopy (background theory)

Knowledge of the heavy metal binding to the clay minerals is of fundamental importance to predict the stability of the metal compound formed. Several methods are available but their complications do limit their use. Infrared spectroscopy is often used in a qualitative way to identify substances and characteristic groups. Finger print techniques and group frequencies are then used to recognize specific pattern of the vibrational energies. Molecular vibrations are also sensitive and useful for comparisons of changes in the bond character in different complexes. However, in order to make detailed interpretations of the chemical bonding, analyses accounting for all possible vibrational modes and their interactions in the molecules should be performed and this is generally a very complicated task. In this work, Extended X-Ray Absorption Fine Structure (EXAFS) was used to characterize metal sorbed species on the PTC surfaces and in the Moringa extracts. The main advantages of EXAFS are that all the nearest neighbour distances around the absorbing element are observed and all states of aggregation can be studied with high precision in the distances even in very dilute samples with metals sorbed on mineral or clay surfaces The absorption spectrum at an absorption edge of an element has traditionally been divided into two main regions (XANES and EXAFS) where the EXAFS region refers to the oscillatory structure in the x-ray absorption coefficient starting at energy about 50 eV higher than the threshold energy E<sub>o</sub>. X-ray Absorption Near Edge Structure (XANES) refers to the region within about  $\pm$  10 eV of the

main absorption edge. Theoretical description of the XANES region is still not fully developed. Analysis of the EXAFS region provides such information as type of atoms in the coordination shell and the coordination geometry around the central atom of interest. Figure 10 is an illustration of the two regions for Cr(III) K-edge spectrum.

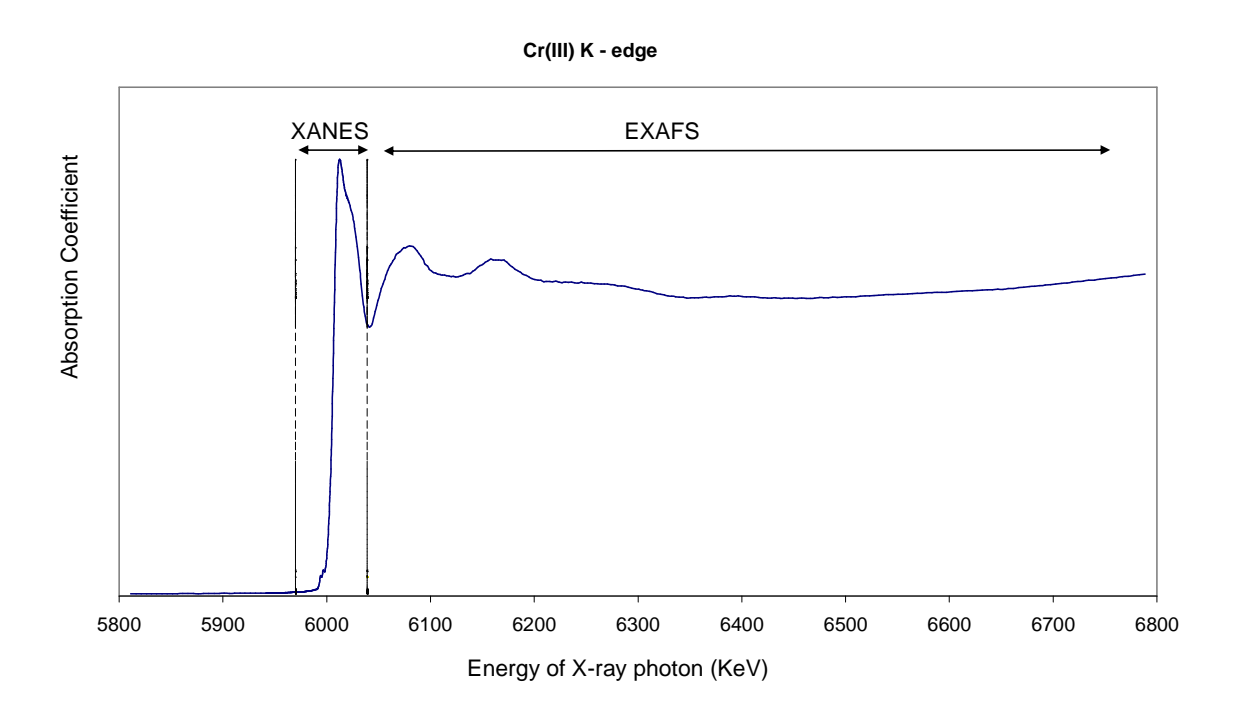


Figure 10: Absorption coefficient as a function of energy; example of the Cr(III) K – edge spectrum of chromium(III) sorbed clays distinguishing the XANES and EXAFS regions

The EXAFS measurements involve ionization of an atom, by absorption of an X-ray quantum of one of the innermost electrons. In this process a *photoelectron wave* is produced. This outgoing photoelectron wave can be reflected (backscattered) from the surrounding neighbour atoms. The X-ray absorption spectrum of the metal ion of interest will show oscillations, *extended x-ray absorption fine structure*, above the absorption edge. This is due to the fact that the outgoing photoelectron wave can interfere, constructively or destructively with the backscattered wave. The nature of interference depends on the energy of the initially

incoming X-ray quantum. The energy (wavelength) of the photoelectron can be deduced from the de Broglie equation:

(i) 
$$\lambda_e = h[2m_e(E - E_o)]^{-1/2}$$

where h is the Plank's constant,  $m_e$  is the mass of the electron, E is the energy of the incident X-ray photon, and  $E_o$  the threshold energy of the metal (ion) of interest. The wave vector, k, is:

(ii) 
$$k = \frac{2\pi}{\lambda_e}$$

The scattering process of the photoelectron can be modelled at different levels of scattering theory. The EXAFS oscillation,  $\chi_i(k)$ , is the sum of modified sine waves with different frequency and phase from each backscattering coordination shell j, around the central atom i, and can be written in the general form:

(iii) 
$$\chi_i(k) = \sum_j A_j(k) \sin[\Psi_{ij}(k)]$$

where  $A_j(k)$  is the total backscattering amplitude of the  $j^{th}$  shell of the backscattering atoms and  $\Psi_{ij}(k)$  is the corresponding total phase function. The amplitude and the phase functions contain structural information. A model is therefore constructed with parameters that can be adjusted to improve the fit between the experimental and calculated EXAFS function. A detailed EXAFS function is thus written as:

(iv) 
$$\chi_{i}(k) = \sum_{j} \frac{N_{j}.S_{o}^{2}(k)}{k.R_{j}^{2}} \left| f_{eff}(k) \right|_{j} \cdot \exp(-2k^{2}\sigma_{j}^{2}) \cdot \exp[-2R_{j}/\Lambda(k)] \cdot \sin[2kR_{j} + \phi_{ij}(k)]$$
 where

 $N_{\rm j}$  = number of backscatterers in the  $j^{\rm th}$  shell.

 $R_j$  = distance between the central atom i and the backscatterers in the j<sup>th</sup> shell.

 $S_0^2(k)$  = amplitude reduction factor due to multiple excitations, etc.

 $f_{\text{eff}}(\mathbf{k})$  = effective amplitude function for each scattering path.

 $exp[-2\sigma_i^2k^2]$  = Debye-Waller factor in the harmonic approximation.

 $\sigma_i$  = Debye Waller parameter accounting for thermal and configurational disorder.

 $\Lambda(k)$  = photoelectron mean free path

 $exp[-2R_i/\Lambda(k)] = \text{mean free path factor}$ 

 $[2kR_i + \varphi_{ij}(k)] = \text{total phase} = \psi_{ij}(k)$ 

 $\varphi_{ij}(k)$  = phase shift due to the coulomb potential of the central atom i and of the backscattering atom j

The total phase of the photoelectron wave is a function of both the metal ion – back scatterer distance,  $R_i$ , and the phase shift attained by coulomb potential effect of the backscatter atom. The amplitude is a multi component product of the terms preceding the sinusoidal function in the EXAFS equation (equation iv). The effective amplitude  $f_{eff}(k)$  is calculated for each scattering path and depends on the nature of the backscattering atom. The amplitude reduction factor  $S_0^2(k)$  is related to the absorber and describes the intensity loss in experimental EXAFS data due to numerous excitations of valence electrons. The mean free path factor  $exp[-2R_i/\Lambda(k)]$  expresses the probability after excitation of inelastic scattering or core hole being filled before the photoelectron returns to the absorber. The Debye-Waller factor  $exp[-2\sigma_i^2k^2]$  presents the amplitude loss due to vibrational and configurational disorder (Jalilehvand, 2000). Fourier transformation is used to separate the frequencies of the photoelectron scattered waves and backscattering atoms are identified after correction for phase shift effects. Distances of the backscattering atoms from the central atoms are also calculated by taking into account the intensity and frequency of each elementary wave constituting the EXAFS spectrum. In order to filter overlap of contributions from different backscattered atoms, the Fourier transform spectrum calculated from the EXAFS experimental spectrum is back transformed to generate a Fourier filtered EXAFS spectrum (FT<sup>-1</sup>). The FT<sup>-1</sup> EXAFS spectrum is then compared with theoretical EXAFS spectra, calculated from individual back-scattering paths using, for example, FEFF7 program (FEFF code, 1991-1996). The difference between computed and filtered spectra is optimized using a least-squares approach where the structure parameters in the calculated spectrum is refined versus the experimental data. Figure 11 is an illustration of EXAFS data treatment process. Details of the EXAFS results are explained in Paper(III) and (V).

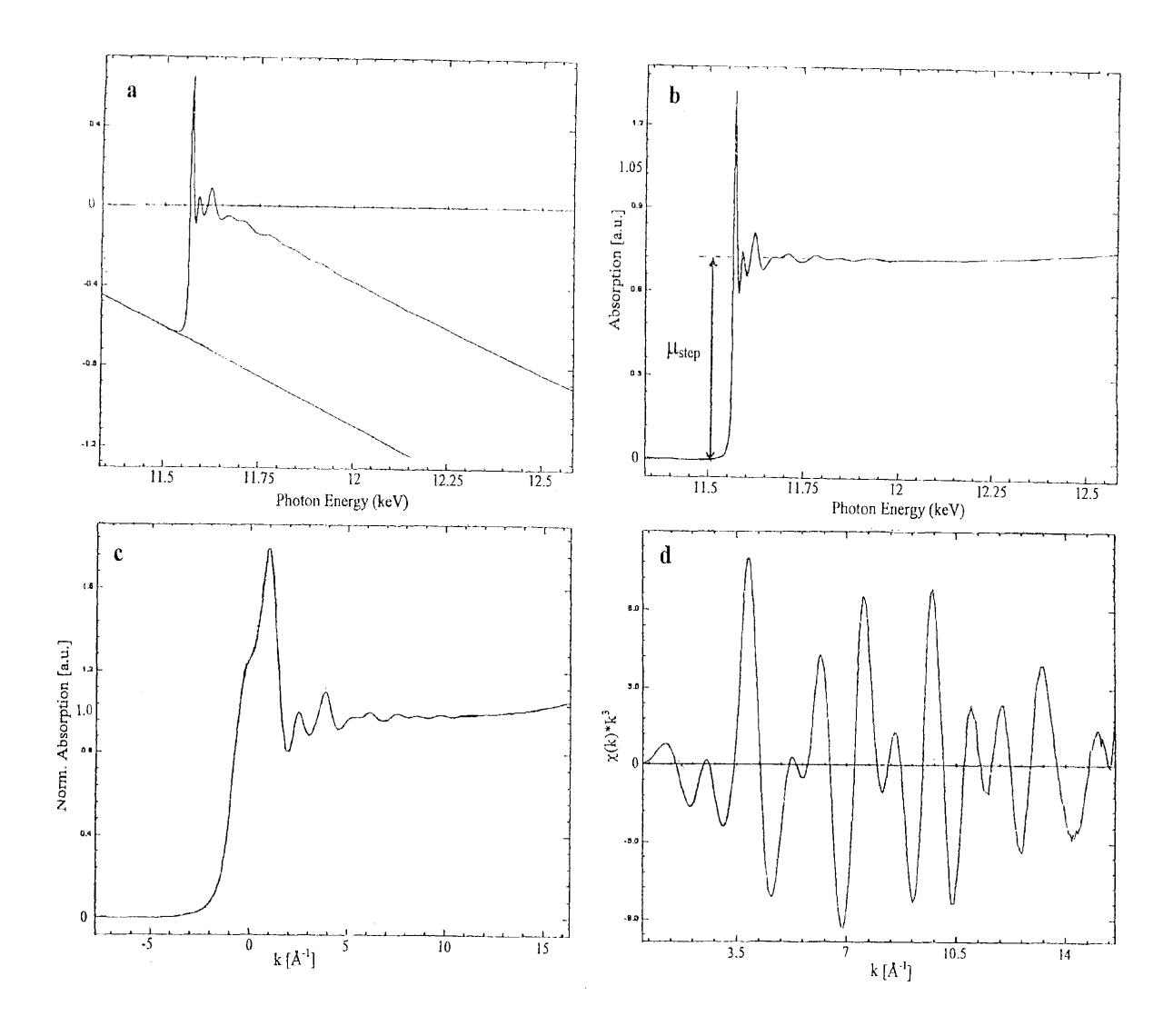


Figure 11: Illustration on extraction of EXAFS oscillation from raw data. a) fit of linear pre-edge background, b) background subtraction, c) conversion of energy to k-space after edge step normalization, d)  $k^3$ -weighted EXAFS oscillation after spline removal.

#### 3.1.9.1 EXAFS sample preparation

20 mmol·dm<sup>-3</sup> copper(II), zinc(II), cadmium(II), and lead(II) solutions were prepared by dissolving analytical grade reagent  $Cu(NO_3)_2 \cdot H_2O$ ,  $Zn(NO_3)_2 \cdot 6H_2O$ ,  $Cd(NO_3)_2 \cdot 4H_2O$ , and  $Pb(NO_3)_2$  respectively in deionized water (reagent sources as explained in Section 3.1.8.1). 20 mmol·dm<sup>-3</sup> chromium(III) solution was prepared by dilution of a 1.4 mol·dm<sup>-3</sup>

Cr(ClO<sub>4</sub>)<sub>3</sub>.6H<sub>2</sub>O stock solution (prepared from chromium(III) perchlorate hexahydrate, Cr(ClO<sub>4</sub>)<sub>3</sub>·6H<sub>2</sub>O in 1.0 mol·dm<sup>-3</sup> hydrochloric acid). 20 mmol·dm<sup>-3</sup> aqueous mercury(II) trifluoromethanesulfonate solution was prepared by dissolving anhydrous Hg(CF<sub>3</sub>SO<sub>3</sub>)<sub>2</sub> in deionized water at pH 2.0 adjusted by addition of nitric acid. 25 mL of the 20 mmol·dm<sup>-3</sup> of the metal solution was added to 1g of the clay and the pH was adjusted to 7.0 by dropwise addition of 1.0 mmol·dm<sup>-3</sup> NaOH for chromium(III), copper(II), zinc(II) mercury(II) and lead(II) clay suspension whereas cadmium(II) clay suspension was adjusted to pH 9.0. The suspensions were stirred for 48 h at room temperature and then centrifuged to separate the rich adsorbed clay samples which were dried in air before the EXAFS measurements. Separate samples at low pH values were also prepared for the EXAFS measurements. The low pH values were 3.2, 4.73, 6.3, 5.4, 2.2 and 4.4 for chromium(III), copper(II), zinc(II), cadmium(II), mercury(II) and lead(II) respectively. For Moringa oleifera water and sodium chloride extracts, 15 mL of the extract was added to 15 mL of 20 mmol.dm<sup>-3</sup> metal solution and the pH was adjusted to about 7. The solution mixtures were stirred for 48 h and then centrifuged at 3000 rpm for 15 min. The metal-rich residues were then dried at room temperature for EXAFS measurements. Lead(II) and mercury(II) solutions were not reacted with the sodium chloride extracts for the chloride ions in the salt extract would have formed stable lead and mercury chloride precipitates respectively. Moringa stenopetala extracts were not prepared for the EXAFS measurements because we had ran short of the seeds then.

#### 3.1.9.2 EXAFS Data collection

Cadmium, chromium and zinc K-edge spectra and mercury L<sub>3</sub>-edge X-ray absorption spectra were collected at the bending magnet beam line 2-3 at the Stanford Synchrotron Radiation Laboratory (SSRL), Stanford, USA, which was operated at 3.0 GeV and a maximum current of 100 mA, and at beam-line I811, MAX-lab, Lund University, Sweden, which was operated at 1.5 GeV and a maximum current of 200 mA. Data collection was performed in transmission and fluorescence mode simultaneously, except for cadmium where only transmission data were collected. The fluorescence measurements were performed with a Lytle detector with a suitable X-ray filter, e.g. vanadium for chromium fluorescence, nickel for copper fluorescence and copper for zinc fluorescence, and with a very gentle flow of argon and/or krypton gas depending on energy. The EXAFS stations were equipped with a

Si[220] (SSRL) or Si[111] (Max-lab) double crystal monochromator. In order to remove higher order harmonics, the beam intensity was detuned to 30, 50, 50, 50, 50 and 80 % for chromium, copper, zinc, mercury, lead and cadmium, respectively, at the end of the scans. Internal energy calibration was made with corresponding metal foil, and in case of mercury with a boron nitride (BN) diluted mercury(II) chloride sample (Thompson *et al.*, 2001). For each sample 3-4 scans were averaged.

The EXAFSPAK program package (George and Pickering, 1993) was used for the data

#### 3.1.9.3 EXAFS Data analysis

treatment. The EXAFS oscillations were obtained after performing standard procedures for pre-edge subtraction, and spline removal. The  $k^3$ -weighted model functions were calculated using ab initio calculated phase and amplitude parameters obtained by the FEFF7 program (FEFF code, 1991-1996). Input to the FEFF7 program was prepared by assuming appropriate angles and distances for solid hexaaquacadmium(II) perchlorate (Johansson and Sandström, 1987), diammonium hexaaquachromium(III) pentafluoride (Marsh and Herbstein, 1983), mercury(II) oxide (Voronin and Shchennikov, 1989), bisaquatetratrifluorosulfonatomercury(II) (Molla-Abbassi et al., 2002), strontium tetrahydroxozincate hydrate, Sr[Zn(OH)<sub>4</sub>]·H<sub>2</sub>O, (Stahl and Jacobs, 1997) and zinc(II) oxide (Albertsson *et al.*, 1989). The standard deviations for the refined parameters were obtained from  $k^2$  weighted least squares refinements of the EXAFS function  $\chi(k)$ , and did not include systematic errors of the measurements. These statistical error estimates provide a measure of the precision of the results and allow reasonable comparisons e.g. of the significance of relative shifts in the distances. However, the variations in the refined parameters, including the shift in the  $E_{\rm O}$ value (for which k = 0), using different models and data ranges, indicate that the absolute accuracy of the distances given for the separate complexes is within ±0.01 to 0.02 Å for welldefined interactions.

#### 3.1.10 Sources of Moringa seeds.

Dry *M. oleifera* seeds were collected from locally naturally growing plants in villages around Chikwawa Boma in Southern Malawi. Dry *M. stenopetala* seeds were purchased from Whizpop Products Ltd, Nairobi in Kenya. The seeds were stored at room temperature.

### 3.1.11 Preparation and characterisation of the Moringa seeds for heavy metal removal experiments

Deshelling of the seeds was done just before extraction of the coagulant by hand. The deshelled seeds were washed in distilled water to remove any dirt, dried in air and then powdered by grinding. Defatting was done by mixing the powder in 95% ethanol (10% w/v) and shaking for 30 min. The solids were separated by centrifugation and dried at room temperature. Coagulant extraction was done by mixing the dried defatted powdered with distilled water and 0.6 mol·dm<sup>-3</sup> NaCl, at 5% (w/v) solutions. The solutions were stirred for 30 minutes and filtered; first, through Munktell filter paper No. 3 and then through 0.47 µm filter. The filtrates are termed crude extracts abbreviated as MOC-DW, MOC-SC, MSC-DW and MSC-SC for the M. oleifera crude extracts of distilled water, sodium chloride, M. stenopetala crude extracts of distilled water and sodium chloride respectively. Ideally the water and salt sodium chloride extracts should have been purified, for example, by using High-trap CM FF1 ml cation exchanger column (Gebremichael et al, 2005) or anionic exchanger packed with 12.2 ml of Amberlite IRA-900 (Okuda et al, 2001). In this work, purification of the extracts was not done due to resource limitation and therefore this section on *Moringa* potential in heavy metal removal can be considered to be in its preliminary stage. However, in order to have an idea of available functional groups in the *Moringa* extracts, proton nuclear magnetic resonance data (<sup>1</sup>H-NMR) of both MS and MO powder were recorded in a Bruker spectrometer DRX-400 operating at 400 MHz. About 10 mg of the powder was dissolved in 1 mL of D<sub>2</sub>O and filtered to remove any undissolved suspending solids before running the NMR experiment.

### 3.1.12 pH profile studies for chromium(III), copper(II), zinc(II) and cadmium(II) sorption

Chromium(II), copper(II), zinc(II) and cadmium(II) stock solutions were prepared as described in section 3.1.8.1. 9.0 mL of 0.1 mol·dm<sup>-3</sup> NaNO<sub>3</sub> was pipetted into each of 10 centrifuge tubes. An appropriate amount of acid (20 mmol·dm<sup>-3</sup> HNO<sub>3</sub>) or base (20 mmol·dm<sup>-3</sup> NaOH) was added to a certain pH (pH<sub>initial</sub>). 1.0 mL of the *Moringa* crude extract (MOC-DW, MOC-SC, MSC-DW or MSC-SC) and 0.5 mL of stock metal solution were added into each of the centrifuge tube. The solution mixtures were shaken for 48 h and then centrifuged for 15 min at 3000 rpm using KUBOTA KS-5200C centrifuge. 3-4 mL of the supernatant was taken, acidified with a drop of concentrated nitric acid and analyzed for the given metal concentration on an atomic absorption spectrophotometer (Perkin Elmer AAnalyst 100). The pH of the remaining supernatant in the centrifuge tubes was recorded as the equilibrium solution pH (pH<sub>equil</sub>). Percentage metal uptake (%E) was calculated by use of equation (3) above (Section 3.1.8.2).

#### 4. RESULTS AND DISCUSSION

This chapter gives a summary of major results of the study.

# 4.1 Quality of water from streams and wastewater treatment plants of Blantyre City (Paper I)

The study provided recent data of concentrations of sodium(I), potassium(I), chromium(III), manganese(II), iron(II), nickel(II), copper(II), zinc(II), cadmium(II), lead(II), nitrates, phosphates and sulphates of water samples of three major streams in Blantyre City (Limbe, Mudi and Nasolo streams) and two wastewater treatment plants in the city (Soche and Limbe WWTPs). The pH, TDS and BOD<sub>5</sub> were also included in this study. The mean values (± SD) of the analysed parameters are presented in Tables 7 and 8. The values were compared to the World Health Organization (WHO, 2004) and the Malawi Bureau of Standards (MBS, 2005) drinking water guidelines.

## 4.1.1 Concentrations/values of pH, total dissolved solids (TDS) and biochemical oxygen demand ( $BOD_5$ )

The pH values were between  $6.63\pm0.14$  and  $9.38\pm0.20$ . Except for the final effluent of Limbe WWTP (pH = 9.38), the pH data for the rest of the sites fell within the recommended standards (pH = 6.5 - 8.5). The high pH observed in treated wastewater at Limbe WWTP could result from production of hydroxyl ions during photosynthesis. Limbe WWTP uses pond system. Algal bloom and water hyacinth were observed in the treatment ponds. These plants use dissolved carbon dioxide or dissolved carbonates and bicarbonates as their source of carbon to produce carbohydrates, oxygen and hydroxyl ions which increase the pH.

Table 7: Concentrations of metal cations in water samples

Parameter	Sampling points										
	1A	1B	2A	2B	3A	3B	4A	4B	5A	5B	WHO (2004)
Pb (mg/l) x ± SD	0.056±0.021	0.090±0.012	0.118±0.013	0.116±0.012	0.030±0.006	0.104±0.068	ND	0.051±0.042	0.027±0.019	ND	0.01m/L
Cd (mg/l) x ± SD	0.011±0.001	0.010±0.004	0.002±0.001	0.015±0.013	0.009±0.014	ND	ND	0.012±0.008	0.009±0.006	0.005±0.006	0.003mg/L
Zn (mg/l) x ± SD	0.340±0.096	0.236±0.026	0.123±0.071	0.630±0.274	0.244±0.101	0.324±0.013	0.166±0.014	0.280±0.093	0.257±0.00	0.234±0.004	*3 mg/L
Cr (mg/l) $x \pm$ SD	.041±0.006	0.048±0.007	0.013±0.000	0.479±0.048	0.089±0.005	0.035±0.005	0.021±0.006	0.054±0.002	0.037±0.006	0.055±0.004	0.05mg/L
Fe (mg/l) $x \pm$ SD	0.942±0.139	0.837±0.283	2.383±0.407	7.280±2.978	1.438±0.247	0.761±0.278	1.761±0.114	1.987±0.203	1.852±0.090	3.071±0.172	*1-3mg/L
Cu (mg/l) x ± SD	0.037±0.031	0.011±0.001	0.014±0.006	0.046±0.011	0.031±0.020	0.018±0.007	0.010±0.000	0.006±0.002	0.025±0.004	0.010±0.006	2mg/L
Ni (mg/l) $x \pm$ SD	0.123±0.034	0.234±0.025	0.282±0.074	0.338±0.106	0.258±0.050	0.183±0.023	0.190±0.013	0.202±0.023	0.206±0.072	0.176±0.078	0.02mg/L
Mn (mg/l) x ± SD	0.072±0.008	0.045±0.004	0.274±0.008	0.460±0.058	0.058±0.007	0.060±0.005	0.184±0.019	0.423±0.007	0.283±0.002	0.747±0.015	0.4mg/L
Na (mg/l) x ± SD	42.00±2.24	43.58±4.05	32.15±1.93	56.33±4.53	34.02±6.87	35.95±2.92	18.93±2.82	98.17±7.83	22.03±1.33	21.48±0.76	*200 mg/L
K (mg/l) $x \pm SD$	15.60±0.61	14.46±2.85	15.10±1.01	16.22±0.93	17.38±3.16	38.30±9.05	4.37±1.16	14.70±3.96	5.60±0.46	9.00±1.37	

x mean value (n = 3)

Sample codes: 1A = Limbe WWTP (Raw), 1B = Limbe WWTP (Final), 2A = Nasolo River (at Grace Bandawe Foundation center),

2B = Nasolo River (at SR Nicolas), 3A = Soche WWTP (Raw), 3B = Soche WWTP (Final), 4A = Limbe Stream (at Mpingwe Sports Club),

SD standard deviation

<sup>\*</sup> suggested but not approved guidelines

**<sup>4</sup>B** = Limbe stream ( at Kara Mansion), **5A** = Mudi River (at MDI), **5B** = Mudi River (at SR Nicolas)

Table 8: Mean values/concentrations of pH, phosphates, nitrates, sulphates, total dissolved solids and biochemical oxygen demand.

Sampling	Parameters									
sites	pН	PO <sub>4</sub> <sup>3-</sup>	$NO_3$	$SO_4^{2-}$ (mg/l)	TDS	$BOD_5$				
		$(mg/l) x \pm$	$(mg/l) x \pm$	$x \pm SD$	$(mg/l) x \pm$	$(mg/l) x \pm$				
		SD	SD		SD	SD				
1A	7.27±0.14	0.79±0.93	2.38±0.15	20.71±0.068	300±8	327±12				
1B	9.38±0.20	0.63±0.23	1.50±0.26	22.90±0.54	269±22	53±3				
2A	7.49±0.01	1.28±1.16	20.18±2.29	22.24±0.67	371±23	66±2				
2B	6.91±0.02	3.20±0.69	0.81±0.12	22.24±1.75	412±14	267±23				
3A	6.63±0.14	5.39±0.66	0.95±0.11	24.52±0.95	291±12	473±12				
3B	7.43±0.03	3.86±0.76	11.66±1.23	39.68±0.54	385±7	33±6				
4A	7.02±0.03	2.60±0.23	5.89±0.39	14.90±1.88	244±17	6±1				
4B	6.98±0.20	3.42±0.00	0.95±0.04	109.72±20.0	586±8	27±1				
5A	7.23±0.03	3.09±0.00	5.14±0.04	42.25±0.13	271±19	17±1				
5B	6.77±0.08	5.50±3.20	0.86±0.06	19.00±1.48	247±9	33±3				
WHO	6.5-8.5	0.5 mg/L	50 mg/L	250 mg/L	*1000	20 mg/L				
(2004)					mg/L	(MBS,				
						2005)				

TDS values ranged from 247 mg/L to 586 mg/L, which were within the set WHO guidelines. However, the TDS levels of water at Soche WWTP (final effluent) (p = 0.0026) and Mudi stream at SR Nicholas (p = 0.0001) were significantly higher than those for Soche WWTP (raw wastewater) and Mudi stream at MDI. TDS indicates the general nature of water quality or salinity. Water with TDS value more than the suggested 1000 mg/L is considered undesirable for domestic uses. The TDS results obtained in this study were much higher than those reported by Lakudzala *et al* (1999), on some points of the Mudi stream. The difference could be due to the sampling techniques used in both studies. In both cases grab sampling technique was used; hence, the reported results were applicable only at the time of sampling. Increased addition of chemicals into the stream from the surrounding industries during the earlier work by Lakudzala *et al* (1999) could therefore account for the high TDS values.

BOD<sub>5</sub> was found to be higher than the Malawi Bureau of Standards (MBS) effluent standard (20 mg/L) at all sampling points except for Limbe stream at Mpingwe and Mudi stream near MDI. The BOD<sub>5</sub> levels obtained in Mudi stream near SR Nicolas were much lower than those by Kuyeli (2006). Kuyeli (2006) reported BOD<sub>5</sub> values of greater than 300 mg/L at the

same point compared to our values of about 33 mg/L in 2005 and this could be attributable to increased informal discharge of organic effluents into the stream by the surrounding industries. BOD<sub>5</sub> is used as a fair measure of cleanliness of water on the basis that values less than 2 mg/L are considered lean, 3 mg/L fairly clean, 5 mg/L doubtful and 10 mg/L definitely bad and polluted (Izonfuo and Bariweni, 2001). The results therefore show that streams in Blantyre get heavily polluted after passing through industrial areas. Although the BOD<sub>5</sub> values at wastewater treatment plants indicate significant reduction after the treatment processes the final effluent values were outside the recommended limit.

#### 4.1.2 Concentrations of metal cations

Lead concentrations were high at Limbe WWTP (both in the raw wastewater and the final treated wastewater, 0.056 to 0.090 mg/L), Nasolo Stream (before and after industrial area, 0.116 to 0.118mg/L) and Soche WWTP (final treated wastewater, 0.104 mg/L). The values were much higher than the given WHO drinking water guideline of less than 0.01 mg/L. Although the study did not look at pollution sources in terms of specific activities taking place in the given areas, suggestions of the sources are however made in this work. Possible sources of the lead contamination are leaching of lead compounds into the streams from uncontrolled disposal of contaminated wastes in the city. Lead is used in storage batteries where an alloy of 91% lead and 9% antimony forms the supporting grid for the oxidizing agent (PbO<sub>2</sub>) and the reducing agent (spongy lead). It is likely that these batteries are simply disposed after use instead of being recovered and recycled. Lead is also used in solders, fusible alloys, bearing metals, pigments and chemicals. During the study, Malawi was still using 'leaded petrol' (petrol in which tetraethyl-lead or tetramethyl-lead has been added as antiknocks). The lead released in the vehicular emissions could be deposited on surrounding water bodies and soils. This could be a major contributing factor to the high lead concentrations at Mudi (near MDI) because the sampling point was under a bridge on a high traffic road. Lakudzala et al (1999) also reported high lead concentrations at Mudi confluence with Nasolo stream.

Cadmium was detected at most of the sampling points ranging from 0.002 to 0.015 mg/L. Most of the values were above the WHO guideline ( 0.003 mg/L). Cadmium, in the recent past, has been mainly used for protective coatings on steel. Although cadmium coatings are being replaced, it is common to find cadmium coated materials in Malawi. Disposal of such materials could be contributing to the high concentrations of cadmium in the streams. Cadmium is also used in small quantities in alloys and batteries and some of its compounds are used in polyvinyl chloride (PVC) products to prevent degradation. There were increases in cadmium concentrations of the stream water after passing through industrial areas (Nasolo and Limbe streams) suggesting that there could be contribution of cadmium contamination from the industries through discharge of incompletely treated wastewater.

Zinc concentrations varied between 0.166 and 0.630 mg/L which were below the WHO suggested limit (3 mg/L). There were no significant differences between points of the same stream or WWTP at the 95% level of confidence. The highest concentration (0.630 mg/L) was observed for Nasolo stream (after passing through industrial site). This could have resulted from a suspected broken sewer line during the sampling.

Chromium levels varied from 0.013 to 0.479 mg/L with values above the WHO guideline of 0.05 mg/L recorded at Soche WWTP raw wastewater (0.089 mg/L), Nasolo (0.479 mg/L), Limbe (0.054 mg/L) and Mudi streams after passing through industries. Chromium is mainly used in the production of non-ferrous alloys and chromium plating. High concentrations of hexavalent chromium (up to 56 mg/l) have been determined in matchstick production effluent in the city where potassium dichromate is used as an oxidizing agent (Kuyeli, unpublished). Such effluents may end up in streams; hence, the identified chromium pollution

Concentrations of iron were between 0.761 and 7.280 mg/L. There was a significant increase in Nasolo River after the industrial area due to the suspected broken sewer line (p = 0.0478) and also in Mudi stream after the industrial area (p = 0.0004). Significant iron level reduction was observed at Soche WWTP (p = 0345) probably due to coagulation processes during the wastewater treatment. Soche WWTP is a conventional biological filter plant; hence, there

could be natural coagulation of the iron on the stones of the trickling filters. Iron has a lot of uses particularly in a wide variety of steels; hence, its absolute concentrations even in natural water bodies tend to be higher than the concentrations of heavy metals such as lead and cadmium. Iron is also an essential element; therefore, its guideline limit in drinking water is quite high (1-3 mg/l).

Nickel concentrations ranged from 0.123 mg/L to 0.338 mg/L and they were all well above the WHO guideline (0.02 mg/L). Nickel is used in both ferrous and non ferrous alloys. Electroplated nickel is an ideal undercoat for electroplated chromium and smaller amounts of nickel are used as catalyst in the hydrogenation of unsaturated vegetable oils and in storage batteries. Uncontrolled disposal of nickel containing effluents from industries could contribute to these high concentrations of nickel.

Manganese concentrations ranged from 0.045 mg/L to 0.747 mg/L. The concentrations for Nasolo stream, Limbe stream and Mudi stream (after passing through industrial areas) were higher than the WHO guideline (0.4 mg/L). Significant manganese level increases were observed in all the streams after passing through industrial areas and reduction at Limbe WWTP after wastewater treatment. Almost all steels contain some manganese which increases the hardness of the steel. Wastewaters from production of steels could therefore be a source of manganese pollution in the water bodies.

Sodium concentrations at all sites were within the suggested WHO maximum limit of 200 mg/L above which the water may have unacceptable taste. Significant increases in sodium levels were noted after Mudi and Nasolo streams had passed through industries which could due to addition of sodium salts to the streams by the industries. Potassium concentrations ranged from 5.60 mg/L to 38.30 mg/L with notable increased levels in water of Soche WWTP (final effluent), Limbe stream (after passing through industrial area) and Mudi stream (after passing through industrial area).

#### 4.1.3 Concentrations of nitrates and phosphates

The concentrations of nitrates and sulphates at all sampling points were lower than the safe limits for drinking water, 50 mg/L and 250 mg/L respectively (WHO, 2004); thus, indicating that there was no danger due to nitrates and phosphates to the water consumers.

Nitrate concentrations were significantly reduced after wastewater treatment at Limbe WWTP but an increase was observed (from 0.95 to 11.66, p = 0.0001) at Soche WWTP. The nitrate reduction at Limbe WWTP could be due to direct uptake by phytoplankton (Lai and Lam, 1997) in the stabilization ponds. Since Soche WWTP is a conventional biological filter plant, organic forms of nitrogen in domestic wastes (influent at the plant) are decomposed by bacteria to ammonium ions which are then oxidized to nitrate (Walstad, 2003); hence, the increase in nitrate concentration at the Soche WWTP.

Phosphate concentrations were significantly above the safe limit of 0.5 mg/L (WHO, 1963). The high phosphate levels may be due to leaching of agricultural wastes including fertilizers into the streams (since there were extensive farming activities along the river banks during the study). It is also possible that the use of phosphate additives in detergent formulations which get leached into the streams through wastewaters generated industrially, domestically or from cloth dyeing and garment industries operating within the city may contribute to the high concentrations of phosphates.

# 4.2 Characterisation and metal sorption studies of the mixed alkaline clays (Paper II and III)

#### 4.2.1 Clay characterisation

The powder x- ray diffraction patterns for both the raw and purified alkaline Tundulu clays (RTC and PTC respectively) are shown in Figures 12 and 13. The analysis of the d-values for the peaks point at an occurrence of illite, disordered kaolinite and carbonate fluoroapatite (JCPDS, 1974: 21-145; 19-272). The kaolinite is said to be disordered because of the weak reflection at d-value of 7.17 Å which is quite intense in well crystallized kaolinite (Brindley

and Brown, 1980). The carbonate fluoroapatite reflections at d values of 2.78, 2.68 and 2.24 Å are all weak indicating that fluoroapatite is not the dominant component of the sample. The reflections at 4.32 and 3.33 Å could be due to presence of halloysite which has 1:1 layer structure as kaolinite but differs from kaolinite by having a sheet of water molecules between the layers (Gustaffson et al, 2005). The 3.33 Å peak is rather explained as a third order peak from illite. The broad intense reflections at 12.25 and 9.97 Å indicate that the material could also contain mica, smectite or vermiculite mixed layer (ML) minerals (Brindley and Brown, 1980). The probability for mica occurrence in the clay fraction is quite restricted because mica is a primary phyllosilicate (Gustafsson et al, 2005) and instead illite ought to be abundant. Clearly there must be some kind of ML-minerals especially as there is a prominent peak at 24 Å. Clear evidences for illite are the peaks at 10.00, 5.00 and 3.33 Å. In this case the 9.97 Å peak could be the one from mica. The presence of calcite is detected in the RTC (reflections at 3.03, 2.28 and 2.09Å) but no traces of it in the PTC, which has been treated for removal of calcite and iron compounds. This implies that calcite is fully removed during the clay purification process. Another explanation for a broad peak at 4.46 Å (or 4.47 Å) instead of badly crystallized kaolinite is that it could come from dioctahedral mica with a peak in the interval 4.45 – 4.49 Å. Because there is a peak near 10 Å the probability could be rather high for the occurrence of a mica peak at 4.46 Å. Potentiometric titrations of the Tundulu mixed clay indicated that the clay is very alkaline. The initial pH values of the clays were greater than 9 for both the RTC and PTC and concentrations of acib-base active sites,  $\{ \equiv SOH_{tot} \}$ , were  $3.2 \times 10^{-3}$  mol·dm<sup>-3</sup> (5.3×10<sup>-4</sup> mole/g) and  $5.1 \times 10^{-4}$  mol·dm<sup>-3</sup> (8.5×10<sup>-5</sup> mole/g) respectively. The RTC revealed pH buffer properties in the pH region of 4.0 and 6.0 and also in the region of 7.0 and 8.0. The buffering property in the range of 4.0 to 6.0 could be attributed to low water soluble organic acids such as oxalic, citric, formic and lactic acids (Anonymous, 2005). Deprotonation of water soluble carboxylic groups of humic acids could also contribute to buffering in this range (McBride, 1994). In the pH region of 7.0 to 8.0, buffering property could mainly be attributable to soluble inorganic phosphates (since dihyrogen phosphate has a pKa of 7.2) (Anonymous, 2005). These water soluble organic and inorganic acids were removed during the purification processes; hence, the absence of buffering properties in the PTC sample. However, the PTC curve in the pH region of 4.45 to 7.0 was not as smooth as it would have been in the case of absolute absence of any water soluble acids. This seems to suggest that some reactions occurred contributed to dissolutions and deprotonation of small amounts of acids retained from the purification processes. In addition to the clay minerals, the presence of organic matter in the RTC probably rendered the RTC more effective at cation adsorption than the PTC (McBride, 1994).  $pH_{PZC}$  values were 9.94 and 9.66 for the PTC and RTC respectively which was consistent with the high alkaline nature of the clays.

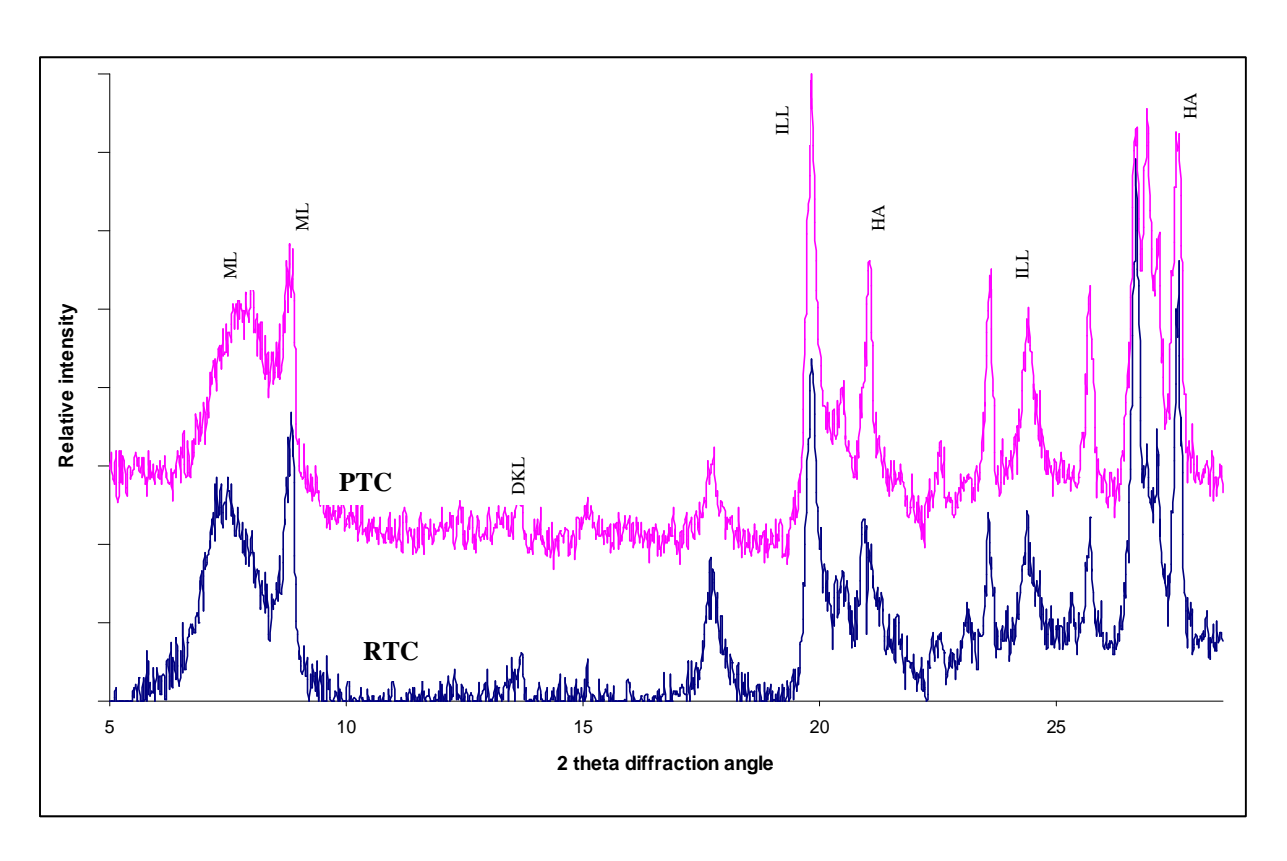


Figure 12: PXRD patterns of Raw Tundulu Clays (RTC) and Purified Tundulu Clays (PTC). ML = Mixed clay mineral , DKL = Distorted kaolinite, HA = Halloysite, ILL = Illite

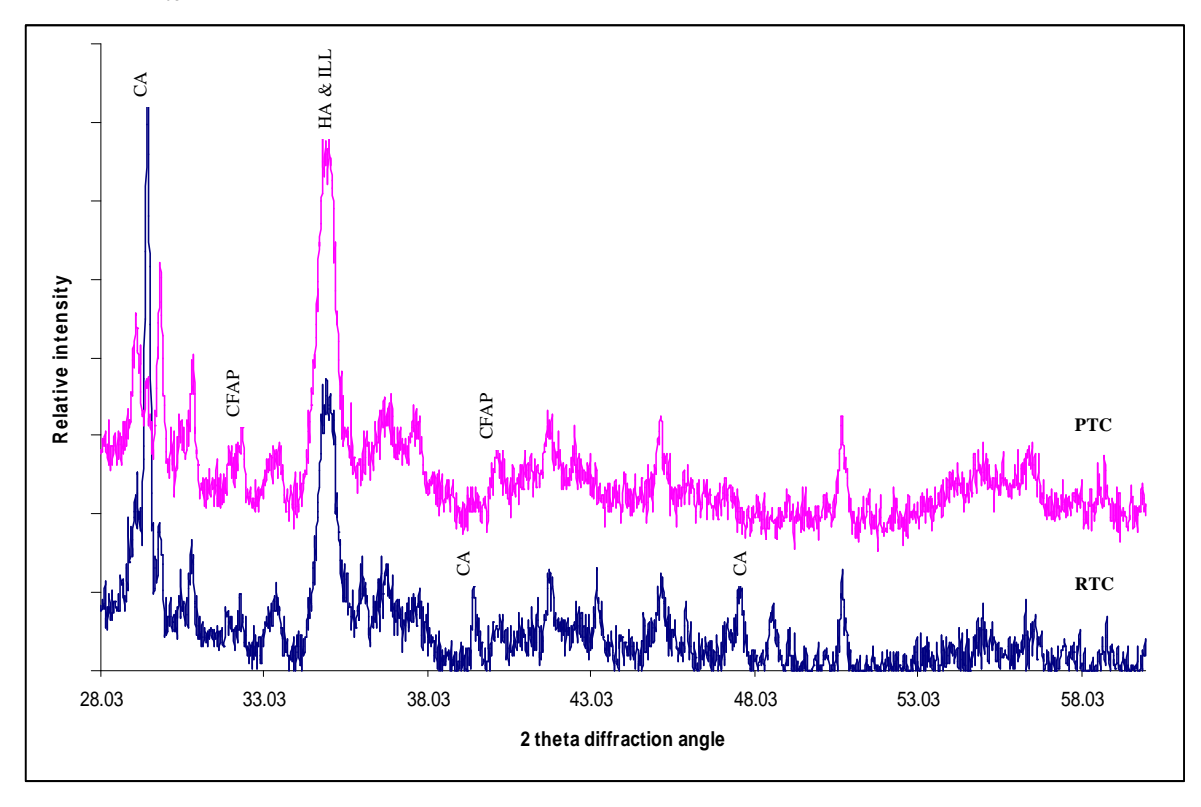


Figure 13: PXRD patterns of Raw Tundulu Clays (RTC) and Purified Tundulu Clays (PTC). CA = Calcite, CFAP = Carbonate fluoroapatite, HA = Halloysite, ILL = Illite

### 4.2.2 Effect of pH on metal sorption by the mixed alkaline clay and structural determination

Mixed alkaline clays (1.43 g/L) have shown to completely remove chromium(III), copper(II), zinc(II), cadmium(II), mercury(II) and lead(II) cations from aqueous solutions within specific pH ranges for each metal solution. The results indicated that 100% chromium(III) removal was achieved between pH 3 and 5 (initial concentration of 5.2 mg/L). Copper(II) removal from (initial concentration of 3.8 mg/L) was achieved between pH 4 and 6.8 (from about 20% to 100%). About 92% of zinc(II) removal (from initial concentration of 3.9 mg/L) was achieved at pH 7.58. Only 90% removal of cadmium(II) (from initial concentration of 3.4 mg/L) was attained even at high pH of 10. Mercury(II) sorption was almost pH independent with sorption capacity fluctuating between 30 and 60 %. Using an initial solution concentration of 4.9 mg/L, complete sorption of lead(II) cations was achieved at pH of about 7.5. Clearly most of the metal sorption processes occurred below the  $pH_{PZC}$  of the clay indicating formation of inner sphere complexes and/or an irreversible absorption process (Stumm, 1992). Insignificant sorption of arsenate was observed at all pH values. Since clay minerals are either neutral or do posses permanent negative charges (Gustafsson et al, 2005), their cation exchange capacity is a result of the permanent negative charge or the acid base reactions of their surface hydroxyl groups. Since As<sup>5+</sup> occurs as H<sub>3</sub>AsO<sub>4</sub>, H<sub>2</sub>AsO<sub>4</sub>, HAsO<sub>4</sub><sup>2-</sup> and AsO<sub>4</sub><sup>3-</sup> in the pH ranges below 2, 3-6, 8-10 and above 12, respectively (Gustafsson et al, 2005, it is not surprising that the clay-arsenic interactions were not favourable for adsorption.

The clay minerals used in this work are classified as either 1:1 or 2:1 clay minerals (Section 4.2.1). Kaolinite (Al<sub>2</sub>(OH)<sub>4</sub>(Si<sub>2</sub>O<sub>5</sub>)) is an example of 1:1 clay mineral which is composed of silica tetrahedral layer (Si<sub>2</sub>O<sub>5</sub>) bonded to aluminium octahedral layer (Al<sub>2</sub>O<sub>4</sub>(OH)<sub>2</sub>) forming a sheet. The sheets are held together by hydrogen bonding resulting in a non-expandable structure. Illite, which is a typical 2:1 clay mineral, comprises sheets built from two silica tetrahedral layers sandwiching aluminium octahedral layer. The sheets are held together by weak van de Waals forces making it easy for other chemical species to enter the interlayer region (Harter, 1998). There are three types of crystalline surfaces onto which metal adsorption can occur on the clays: a hydroxyl plane associated with the alumina octahedral layer, an oxygen plane on the silica tetrahedral layer and particle edges formed from the

incomplete or irregular lattice structure. 2:1 clay minerals have permanent negative charge due to isomorphous substitution of aluminum(III) for silicon(IV) in the silica layer or magnesium(II) for aluminum(III) in the alumina layer (Gustafsson *et al*, 2005). The pH<sub>PZC</sub> of this mixed clay was 9.94 and its cation exchange capacity was 19.73 cmol<sub>c</sub>/Kg (Section 4.2.1). The high pH<sub>PZC</sub> indicate that the surfaces are highly alkaline and this could influence metal hydrolysis and precipitation as additional metal sorption mechanisms (Baes and Mesmer, 1986). Given the heterogeneous nature of the clays it is likely that several metal sorption mechanisms take place simultaneously making the determination of metal/clay component interaction difficult on such material.

Our EXAFS studies of the metal sorbed clays showed that the high alkalinity of the clays promoted hydrolysis of the heavy metals which then precipitated and got sorbed on the surface. In all cases it was shown that oxygen atoms occupy the first shells of the metal atoms on the surface (Paper III). In the sorption of chromium(III) cations, presence of the trimer, [Cr<sub>3</sub>(OH)<sub>4</sub>(H<sub>2</sub>O)<sub>10</sub>]<sup>5+</sup>, was detected at pH 3.24. The formation of indefinite <Cr(OH)<sub>2</sub>Cr(OH)<sub>2</sub>Cr> chains with double hydroxo bridges where each chromium also binds two water molecules/hydroxide ions fulfilling an octahedral configuration was identified at high pH. This shows that such polymeric structures precipitate out and/or get sorbed onto the clay surfaces. EXAFS analysis of copper(II) treated clays both at pH 7 and pH 4.7 indicated an inner sphere octahedral first shell of oxygen atoms with Jahn-Teller distortion and Cu-P average distances of 3.12 Å. The corresponding 3-leg Cu-O-P scattering distance of 3.23 Å was also obtained. These results suggest that the copper(II) is sorbed to the clay mixture through the phosphate groups of the non-clay component of the mixture, fluoroapatite. In the study of copper(II) sorption mechanism on kaolinite, Hyun and Hayes (2004) showed formation of outer sphere surface complex with a tetragonally distorted CuO6 octahedral structure. Polymeric ZnO<sub>4</sub> edge sharing tetrahedral species were observed on the clay surfaces suggesting that precipitation is the mechanism through which zinc(II) species are sorbed on the alkaline clay surface at low and high pH values. In the sorption of cadmium(II) cations it was found that mononuclear precipitate species with octahedral CdO<sub>6</sub> configuration were formed on the clay surfaces. However, it was unclear whether the cadmium(II) ion was sorbed to the clay surface as the hydrated ion or if it was partly hydrolysed based on the

EXAFS data. Formation of cadmium surface precipitate has also been observed on montmorillonite at high pH by Takamatsu *et al.* (2006). Their EXAFS study on sorption of cadmium ions on montmorillonite revealed two sorption types, an outer sphere complex at low pH and surface precipitate at high pH. The EXAFS analysis of the cadmium treated clay at pH 5.4, in this study was not performed because the Cd K-edge (26711 eV) is above the beam energy range at Max-Lab where all the other samples at low pH were analysed. It was observed that the clays affect the speciation of mercury(II) which was easily hdrolysed and sorbed as linear mercury(I), O-Hg-Hg-OH<sub>x</sub> complexes at low pH and mononuclear linear O-Hg-OH<sub>x</sub> (x = 1 or 2) complexes at high pH values. This is contrary to the observation by Brigatti *et al* (2005) who studied sorption of mercury(II) on montmorillonite and vermiculite and found that Hg-O (montroydite-like) structure was formed on both surfaces at low pH instead of the reduced linear mercury(I) in this work.

# 4.3 Sorption of heavy metal cations in crude water and sodium chloride extracts of *Moringa oleifera* and *stenopetala* (Papers IV and V).

The sorption of chromium(III), copper(II), zinc(II) and cadmium(II) to different forms of *Moringa* crude extracts as a function of pH is presented in paper(IV). Generally, metal binding increased with rising pH. The chromium(III) removal mostly occurred between pH 3 and 5 with *M. stenopetala* extract showing better sorption capacity at each pH value than the extracts of *M. oleifera*. Two stages of copper(II) sorption were observed with all extracts; the first stage occurred between pH 4 and 6 and then when pH was raised to above 8. Above this pH (8), sorption of copper(II) in water extracts of *M. stenopetala* (MSC-DW) and sodium chloride extracts of *M. stenopetala* (MSC-SC) and *oleifera* (MOC-SC) increased to over 80% while sorption in water extracts of *M. oleifera* (MOC-DW) still remained low. Most of zinc(II) sorption in MSC-SC and MOC-SC occurred within a narrow pH range of 4 and 4.5 while zinc(II) sorption started at pH 6 with most of it occurring between pH 6 and 8. The results were consistent with metal ion uptake by most biomasses (Igwe *et al*, 2005). A possible mechanism of metal uptake entails exchange of hydrogen ion at the substrate by the

metal ion (Igwe *et al*, 2005). Such an exchange reaction would therefore be influenced by the relative concentration of the exchangeable hydrogen ion on the substrate and the hydrogen ion concentration (as measured by pH) in the medium. The higher the concentration of acid in the medium (lower pH) the more difficult it is for deprotonation of the substrate; consequently there would be insignificant binding of the metal (Ajmal *et al*, 2000). Characterization of the seed powder by <sup>1</sup>H-NMR gave chemical shifts at 1.2, 1.3, 1.9, 2.8, 4.8, 5.2, 5.4, 5.5 7.1 and 7.4 ppm indicating presence of amide (-CO-N-H), benzenoid (Ar-H), amino (R-NH<sub>2</sub>), saturated and unsaturated alkyl fragments in both *M. oleifera* (MO) and *stenopetala* (MS). A singlet chemical shift at 1.5 ppm in MS, probably due to sulfhydryl (R-SH) fragment, was observed. A forest of peaks between chemical shift 3.2 and 4.2 ppm was observed, which were difficult to assign to any molecular fragments. This may explain why MS showed slightly better metal sorption capacity than MO at most pH values. The heavy metal sorption ability of *M. stenopetala* and *M. oleifera* could thus be attributable to coordination or complex formation between the metal cations and pH dependent oxygen and nitrogen anionic sites of the *Moringa* proteins or free amino acids (Costa *et al*, 1997).

The Hg(II) L<sub>3</sub>-edge EXAFS analysis of water extracts of *M. oleifera* treated with mercury(II) showed a selenium K-edge absorption peak at about 12658 eV revealing presence of selenium in the *Moringa* extracts in addition to the organic fragments observed in the <sup>1</sup>H-NMR study.

The EXAFS function for chromium in the *Moringa* and the corresponding FT (Paper V) fitted very well with hydrolysed chromium (existing either as [Cr<sub>3</sub>(OH)<sub>4</sub>(H<sub>2</sub>O)<sub>10</sub>]<sup>5+</sup> or <Cr(OH)<sub>2</sub>Cr(OH)<sub>2</sub>Cr> ) as was the case with the chromium on clays. The FT showed light back-scatterers, certainly oxygen, at short distance, 1.97 Å, and a heavier back-scatterer, most probably chromium, at ca. 3.0 Å, and a smaller contribution at ca. 3.8 Å, most probably multiple scattering within the expected CrO<sub>6</sub> core. The copper(II) EXAFS spectrum was consistent with an octahedral oxygen shell with Jahn-Teller distortion. The equatorial (within the square planar) Cu-O bond was 1.97 Å whereas the two axial Cu-O bond lengths were 2.29 Å. The goodness of fit parameters improved significantly after adding Cu···C distance and Cu-O-C three - leg scattering path at 2.96 and 3.10 Å, respectively suggesting that the

equatorial oxygens around the Cu were part of carboxylate groups in the *Moringa* extracts whereas the axial oxygens could be from water molecules. The EXAFS spectrum for the mercury(II) treated *Moringa* was dominated by a shell of light-back-scatterers around the mercury at bond length, 2.15 Å. The distance at 2.15 Å was consistent with Hg-N bond of Hg<sup>2+</sup> in amide groups. This indicated that mercury(II) was sorbed on the *Moringa* extracts through nitrogen (probably from amino acids) as the donor atom. The EXAFS spectrum of the Hg treated *Moringa* also showed presence of significant concentration of selenium in the *Moringa* extracts. It would therefore be expected that Hg interacts strongly with selenium since selenium is a soft ligand and Hg is a soft acid (Shriver *et al*, 1992). However, no Hg...Se distances were observed. This indicated that the nitrogen donor groups, in the *Moringa* extracts, are significantly much more than the selenium.

## 5. PRACTICAL APPLICATIONS OF THE WORK, LIMITATIONS, FUTURE RESEARCH AND CONCLUSIONS

It is becoming essential to understand and manage the precious water commodity in a wise and cost effective manner in the world. This work has studied one of the main aspects of water management; namely, pollution control. In order to effectively use a metal adsorbent for the removal of the metal from contaminated water, the adsorbent must satisfy at least three requirements:

- i. metal adsorption must be thermodynamically possible,
- ii. adsorbent must not lead to adverse effects such as introduction of other pollutants including bacterial growth into the treated water, and
- iii. kinetic limitations must not prevent use of the adsorbent even at very short contact time.

Studies in Papers II-V address the first requirement. The identified clay properties, characteristic pH ranges within which the clays and *Moringa* extracts sorb heavy metals, and the sorption mechanisms will assist in design and optimisation of local cost effective heavy metal remediation in contaminated water. The treatment methods may be applicable both at household level by use of clay packed filtration columns and in wastewater treatment plants by dosing of clays at a selected stage of the treatment process. Introduction of adverse effects in treated water is not expected to be a problem since the clays are pre-treated as explained in Section 3.1.4. However further filtration and clarification stages may be needed after treatment if the water is to be used for domestic purposes such as drinking. The extraction of *Moringa* coagulating compounds, rather than direct use of the *Moringa* seed powder or filter cake reduces introduction of high loads of organic compounds that may increase the BOD of the treated water.

The third requirement may be part of pilot studies of the materials. Trials on use of the materials in heavy metal removal using a lab-scale wastewater treatment plant are thus proposed as part of further work. Such trials need to involve dynamic experiments, which include determining the best position for dosing of the clays or *Moringa* (such as at the sedimentation tank or at the tertiary stage of wastewater treatment process) and calculations

of proper flow rates to improve contact time. Further, experiments using columns should also to be carried out to asses the outlet metal concentrations from given inlet concentrations at given column load of the clays or the *Moringa*. The management of the metal containing sludge should be included in future study.

#### The major findings of this study are:

- Water and wastewaters in streams and wastewater treatment plants within the Blantyre City in Malawi contain high levels of heavy metals such as lead, chromium, cadmium, nickel and manganese which may be attributed to discharge of incomplete treated wastewater from industries within the city and agricultural activities along the river banks. Although BOD<sub>5</sub> values at wastewater treatment plants in Blantyre are significantly reduced after the treatment processes the final BOD<sub>5</sub> values of effluents are not within recommended limits.
- The Tundulu alkaline mixed promote surface hydrolysis of the heavy metals within characteristic pH ranges for given metals (pH ranges of 3 to 5 for chromium(III), above 7 for zinc(II), 4 to 8 for copper(II), 6 and 9 for cadmium and above 7.6 for lead(II) ) and their consequent removal. Qualitative mineralogical characterisation of the clays revealed that they contain illite, distorted kaolinite, mixed layer minerals and non-clay mineral carbonate fluoroapatite. The fluoroapatite in the clay mixture enhances the sorption of copper(II) through formation of Cu-O bonds with the oxygen part being contributed by phosphate groups of the apatite
- Sodium chloride and water extracts of *M. oleifera* and *M. stenopetala* have positive heavy metal uptake within characteristic pH ranges (pH above 4 for chromium (III), 6 for copper(II), 4 for zinc(II) and 7 for cadmium(II)).
- EXAFS studies of metal rich *M. oleifera* extracts show that copper(II) interacts with oxygen atoms of carboxylate groups in the extracts while mercury interacts with nitrogen atoms of amide groups. Uptake of chromium by the extracts is through hydrolysis mechanism.

#### REFERENCES

Adhikari, T and Singh M.V (2003). Sorption characteristics of lead and cadmium in some soils of India. *Geoderma*, 114: 81-92.

Aizenberg, I., Miara, L and Ulman, O (2006). Heavy metal toxicity in psittacine birds. *Israel Journal of Veterinary medicine*, 61 (1): 28-29.

Ajmal, M., Rao, R. A. L., Ahmad, R and Ahmad, J (2000). Adsorption studies on Citrus reculata (fruit peel of orange): removal and recovery of Ni(II) from electroplating wastewater. Journal of Hazardous Materials, B79: 117-131.

Albertsson, J., Abrahams, S.C and Kvick, Å (1989). Atomic displacement, anharmonic thermal vibration, expansivity and pyroelectric coefficient thermal dependences in ZnO. *Acta Crystallographica Section B*, 45: 34-40.

Alloway, B.J., Ayres, D. C (1995). Chemical principles of environmental pollution. 2<sup>nd</sup> Edn, Blackie Academic & Professional: London, 190-217.

Ammann, L (2003). Cation exchange and adsorption on clays and clay minerals. PhD thesis, Christian-Albrecht Universität, Kiel: Germany.

Anonymous (1993). Moringa oleifera: A perfect tree for home gardens. http://www.winrock.org/forestry/factnet.htm

Anonymous (1996). Water quality. <a href="http://www.watertechnology.net/glossary/water-quality.html">http://www.watertechnology.net/glossary/water-quality.html</a>

Anonymous (2005). pKa's of inorganic and oxoacids. http://www.chem.wisc.edu/areas/reich/pkatable/index.htm APHA, American Public Health Association, American Water Works Association and Water Pollution Control Federation (1985). Standard methods of the examination of water/wastewater. 16<sup>th</sup> Edn. APHA, AWWA, and WPCF, New York, 143-217, 466-483, 493-498, 543-549

Auboiroux, M. Baillif, P., Touray, J.C and Bergaya, F (1996). Fixation of Zn<sup>2+</sup> and Pb<sup>2+</sup> by a Ca-montmorillonite in brines and dilute solutions: Preliminary results. *Applied Clay Science*, 11: 117-126.

Baes, C. F. Jr and Mesmer, R. E (1986). Hydrolysis of cations. Reprint Edn, Krieger Publishing Company, Malabar, FL, 358-365.

Baig, M.A., Mehmood, B and Matin, A (2003). Removal of chromium from industrial effluents by sand filtration. Electronic Journal of Environmental, Agricultural and Food Chemistry. hhtp://ejeafche.uvigo.es/2(3)2003/005232003F.htm

Barbier, F., Duc, G and Petit-Ramel, M (2000). Adsorption of lead and cadmium ions from aqueous solution to the montmorillonite/water interface. *Colloids and Surfaces. A, Physicochemical and Engineering Aspects*, 166: 153-159.

Barrow, N.J., Bowden, J.W., Posner, A.M and Quirk, J.P (1981). Describing the adsorption of Copper, Zinc and Lead on a Variable Charge Mineral Surface. *Australian Journal of Soil Research*, 19: 309-321.

Bektaş, N., Agim, B.A and Kara, S (2004). Kinetic and equilibrium studies in removing lead ions from aqueous solutions by natural sepiolite. *Journal of Hazardous Materials*, B112: 115-122.

Benjamin, M.M (1983). Adsorption and surface precipitation of metals on amorphous iron oxyhydroxide. *Environmental Science Technology*, 17 (11): 686-692.

Bergaya, F and Vayer, M (1997). CEC of clays: measurement by adsorption of a copper ethylenediamine complex. *Applied Clay Science*, 12: 275-280

Bourlivia, A., Michalilidis, K., Sikalidis, C and Trontsios, G (2004). Removal of lead and zinc from aqueous solutions by adsorption on vermiculite from Askos area in Macedonia (Northern Greece). *Bulletin of the Geological Society of Greece*, Vol. XXXVI.

Breen, C., Bejarano-Bravo, C.M., Madrid, L., Thompson, G and Mann, B.E (1999). Na/Pb, Na/Cd and Pb/Cd exchange on a low iron Texas bentonite in the presence of competing H<sup>+</sup> ion. *Colloids and Surfaces. A, Physicochemical and Engineering Aspects*, 155: 211-219.

Brigatti, M.F., Corradini, F., Franchini, G.C., Mazzoni S., Medici L., and Poppi, L (1995). Interaction between montmorillonite and pollutants from industrial waste-waters: exchange of Zn<sup>2+</sup> and Pb<sup>2+</sup> from aqueous solutions. *Applied Clay Science*, 9: 383-395.

Brigatti, M.F., Colonna, S., Malferrari, D., Medici, L and Poppi, L (2005). Mercury adsorption by montmorillonite and vermiculite: a combined XRD, TG-MS and EXAFS study. *Applied Clay Science*, 28: 1-8.

Brindley, G.W and Brown, G (1980). Crystal structures of clay minerals and their x-ray identification. Mineralogical Society: London, 495 pp.

Chang, W.C., Hsu, G.S., Chiang, S.M and Su M.C (2006). Heavy metal removal from aqueous solution by wasted biomass from a combined As-biofilm process. *Bioresource Technology*, 97: 1503-1503.

Chhabra, R., Pleysier, J and Cremers, A (1975). The measurement of the cation exchange capacity and exchangeable cations in soils: A new method. Proceedings of the International Clay Conference, 1975, 439-449.

Černă, M (1995). Use of solvent extraction for the removal of heavy metals from liquid waste. *Environmental Monitoring and Assessment*, 34 (2): 151-163.

Coles, C.A and Yong, R.N (2002). Aspects of kaolinite characterization and retention of Pb and Cd. *Applied Clay Science*, 22: 39-45.

Costa, G., Michant, J. C and Gucket, G (1997). Amino acids exuded from cadmium concentrations. *Journal of Plant Nutrition*, 20: 883 – 900.

Cullity, B.D (1978). Elements of X-Ray Diffraction. 2<sup>nd</sup>Edn. Addison-Wesley Publishing Company, London, 233-247.

da Fonseca M.G., de Oliveira M.M and Arakaki, L.N.H (2006). Removal of cadmium, zinc, manganese and chromium cations from aqueous solution by a clay mineral. *Journal of Hazardous Materials*, B137: 288-292.

DEA, Department of Environmental Affairs (2002). State of Environment Report 2002. Government of Malawi, Lilongwe: Malawi, 95-111.

Deutsch – Äthiopischer Verin e.V. (2000). Moringacea – Moringa family. <a href="http://www.geocities.com/akababi/mira.pdf">http://www.geocities.com/akababi/mira.pdf</a>

Echeverria, J.C., Zerranz, I., Estella, J and Garrido, J.J (2005). Simultaneous effect of pH, temperature, ionic strength, and initial concentration on the retention of lead on illite. *Applied Clay Science*, 30: 103-115.

Elshazly, A.H and Konsowa, A.H (2003). Removal of nickel ions from wastewater using a cation exchange resin in a batch-stirred tank reactor. *Desalination*, 158: 189-193.

Elzinga, E.J and Sparks, D.L (2001). Reaction condition effects on Nickel sorption mechanism in Illite – suspension. *Soil Science Society of America Journal*, 65: 94-101.

FEFF code for ab initio calculations of XAFS: a. Mustre de Leon, J., Rehr, J.J., Zabinsky, S.I and Albers, R.C (1991). *Physical Review* B 44, pp. 4146, b. Zabinsky, S.I., Rehr, J.J., Ankudinov, A.L., Albers, R.C and Eller, M.J (1995). *Physical Review* B 52, pp. 2995, c. Ankudinov, A.L (1996). Ph. D Thesis, University of Washington, Seattle: USA, 1996.

Gassenschmidt, U., Jany, K.D., Tauscher, B and Niebergall, H (1995). Isolation and characterisation of a flocculating protein from Moringa oleifera Lam. *Biochimica et Biophysica Acta*, 1243: 477-481.

George, G. N., Pickering, I. J (1993). EXAFSPAK - A Suite of Computer Programs for EXAFS Analysis. SSRL, Stanford University, CA., USA.

Ghebremichael, K.A., Gunatha, K.R., Henriksson, H., Brumer, H and Dhalhammar, G (2005). A simple purification and activity assay of the coagulant protein from Moringa oleifera seed. *Water Research*, 39: 2338 – 2344.

Ghasi, S., Nwobodo, E and Ofili, J.O (2000). Hypocholesterolemic effects of crude extract of leaf of Moringa oleifera Lam in high fat diet fed wister rats. *Journal of Ethnopharmacology*, 69: 21-25.

Guevara, A.P., Vargas, C., Sakurai, H., Fujiwara, Y., Hashimoto, K., Maoka, T., Kozuka, M., Ito, Y., Tokuda, H and Nishino, H (1999). An antitumor promoter from Moringa oleifera Lam. *Mutation Research/Genetic Toxicology and Environmental Mutagenesis*, 440: 181-188.

Gupta, M., Mazumder, U and Chakrabarti, S (1999). CNS activities of methanolic extract of Moringa oleifera root in mice. *Fitoterapia*, 79: 244-250.

Gustafsson, J.P., Jacks, G., Simonsson, M and Nilsson, I (2005). Soil and Water Chemistry. Lantbruks Universitet Sveriges (SLU), KTH Arkitektur och samhällsbyggnad, Uppsala, Sweden, 27-63.

Hall, J.L (2002). Cellular mechanisms for heavy metal detoxification and tolerance. *Journal of Experimental Botany*, 53 (366): 1-11.

Harrison, R.M. (ed) (1996). Pollution: Causes, effects and Control. 3<sup>rd</sup> Edn. Royal Society of Chemistry: Cambridge, 480 pp.

Harter, R.D (1983). Effect of soil pH on adsorption of lead, copper, zinc and nickel. *Soil Science Society of America Journal*, 47: 47-51.

Harter, R (1998). Building the phyllosilicates. http://pubpages.unh.edu/~harter/crystal.htm

Hyun, S.P and Hayes, K.F (2004). Copper(II) sorption mechanism on kaolinite: An EPR and EXAFS study. *Journal of Mineralogical Society, Korea*, 12(1): 1-9.

Henry, E., Dembo, E.G., Sajidu, S.M and Zimba G (2004). A preliminary investigation on use of Moringa Oleifera polyelectrolytes for wastewater treatment in Malawi. Proceedings of WAMDEC 2004 28-30 July, Elephant Hills, Victoria Falls, Zimbabwe.

Huheey, J., Keiter, E.A and Keiter, R.L (1993). Inorganic Chemistry. Principles of structure and reactivity. Fourth Edition, HarperCollins College Publishers, 123.

Igwe, J.C., Nwokennaya, E.C. and Abia, A.A (2005). The role of pH in heavy metal detoxification by bio-sorption from aqueous solutions containing chelating agents. *African Journal of Biotechnology*, 4 (10): 1109-112.

Igwe, J.C and Abia, A.A (2006). A bioseparation process for removing heavy metals from wastewater using biosorbents. *African Journal of Biotechnology*, 5 (12): 1167-1179.

Izonfuo, L.W.A and Bariweni, A.P (2001). The effect of urban runoff water and human activities on some phsico-chemical parameters of the Epie Creek in Niger Delta. *Journal of Applied Science and Environmental Management*, 5 (1): 47-55.

Jahn, S.A.A (1981). Traditional Water Purification in Tropical Developing Countries-Existing Methods and Potential Application. Publ 117 Deutsche Gesellschaft für Technische Zusammenarbeit (GTZ) GmbH, Eschborn.

Jahn, S.A.A (1988). Using Moringa seeds as coagulants in developing countries. *Journal of the American Water Works Association*, 80 (6): 43-50.

Jahn, S.A.A (1991). The traditional domestication of a multipurpose tree Moringa stenopetala (Bak.f.) Cuf. in the Ethiopian Rift valley. *Ambio*, 20 (6): 244-247 (E).

Jalilehvand, F (2000). Structure of hydrated ions and cyano complexes by x-ray absorption spectroscopy. Doctoral Thesis, Department of Chemistry, Stockholm, 182 pp.

Janek, M and Lagaly, G (2003). Interaction of a cationic surfactant with bentonite: a colloid chemistry study. *Colloid and Polymer Science*, 281: 293-301.

Järup, L (2003). Hazards of heavy metal contamination. *British Medical Bulletin*, 68: 167-182.

JCPDS (1974). Selected powder diffraction data for minerals. Publication DBM-1-23. Joint Committee on Powder Diffraction Standards, 1601 Park Lane, Swarthmore, Pennsylvania 19081, U.S.A.

Johansson, G., and Sandström, M (1987). The crystal structure of hexaaquacadmium(II) perchlorate, [Cd(H<sub>2</sub>O)<sub>6</sub>](ClO<sub>4</sub>)<sub>2</sub>. *Acta Chemica Scandinavica Series A*, 41: 113-116.

Kadewa, W.W., Henry E.M.T., Masamba, W.R.L and Kaunda C.C (2001). Impact of Sewage sludge application to horticulture: A case study of the City of Blantyre. Proceedings of the first Chancellor College Research Dissemination Conference 28 – 30 March 2001, University of Malawi: Zomba, 271 – 279.

Karadi, R.V., Gadge, N.B., Alagawadi K.R and Savadi, R.V (2006). Effect of Moringa oleifera Lam. root – wood on ethylene glycol induced urolithiasis in rats. *Journal of Ethnopharmacology*, 105: 306-311.

Khan, S.A., Rehman, R and Khan, M.A (1995). Adsorption of chromium(III), and chromium (IV) and silver (I) on bentonite. *Waste Management*, 15 (4): 271-282.

Kumari, P., Sharma, P., Srivastava, S and Srivastava, M.M (2006). Biosorption studies on shelled Moringa oleifera Lamarrck seed powder: Removal and recovery of arsenic from aqueous system. *International Journal of Mineral Processing*, 78: 131 – 139.

Kunze, G.W and Dixon J.B (1986). Pretreatment for mineralogical analysis. pp 99-100. *In* Klute A. (ed.) '*Methods of soil analysis. Part 1: Physical and Mineralogical Methods*' Second Edition, ASA and SSSA, Madison, WI.

Kuyeli S.M (2007). Assessment of industrial effluents and their impact on water quality in streams of Blantyre City, Malawi. MSc thesis, University of Malawi: Zomba, 112 pp.

Lai, P. C. C and Lam, P. K. S (1997). Major pathways for nitrogen removal in wastewater stabilization ponds. *Water, Air & soil pollution*, 94 (1-2): 125-136.

Lakudzala, D., Tembo, K.C and Manda I.K (1999). An investigation of chemical pollution in Lower Shire River, Malawi. *Malawi Journal of Science and Technology*, 5: 87-94.

Lalas, S and Tsaknis, J (2002). Characterisation of Moringa oleifera seed oil variety "Periyakulan 1". *Journal of Food Composition and analysis*, 15: 65-77.

Leuck, M and Kunz, H (1998). Synthesis of active principles from the leaves of Moringa oleifera using s-penta-4-enyl thio glycosides. *Carbohydrate Research*, 312: 33-44.

Lower, S.K., Maurice, P.A., Traina, S.J and Carlson, E.H (1998). Aqueous Pb sorption by hyroxylapatite: Application of atomic force microscopy to dissolution, nucleation, and growth studies. *American Mineralogist*, 83: 147-158.

Lusvardi, G., Malavasi, G., Menabue, L and Saladini, M (2002). Removal of cadmium ion by means of synthetic hydroxyapatite. *Waste Management*, 22: 853-857.

Lutzenkirchen, J (1997). Ionic strength effects on cation sorption to oxides: macroscopic observations and their significance in microscopic interpretation. *Journal of Colloid and Interface Science*, 195: 149-155.

Ma, Q. Y (1994). Effects of aqueous Al, Cd, Cu, Fe(II), Ni, and Zn on Pb immobilization by Hydroxyapatite. *Environmental Science and Technology*, 28: 1219-1228.

Maguire, M., Slaveck J., Vimpany, I., Higginson, F.R and Pickering, W.F (1981). Influence of pH on Copper and Zinc uptake by soil clays. *Australian Journal of Soil Research*, 19: 217-229.

Makkar, H.P.S and Becker, K (1996). Nutritional value and antinutritional components of whole and ethanol extracted Moringa oleifera leaves. *Animal Feed Science Technology*, 63: 211-228.

Malawi Bureau of Standards (2005). Drinking water – specifications, 1<sup>st</sup> revision, MS 214: 2005, 6.

Marsh, R. E and Herbstein, F. H., 1983. Some additional changes in space groups of published crystal structures. Acta Crystallographica Section B, 39, 280-287; Marsh, R. E.,

Herbstein, F. H., 1977. xxxxxxxxx Zeitschrift fur Anorganische und Allgemeine Chemie 436: 29-38.

Masamba, W.R.L and Chimbalanga, R.M (2001). Heavy metal pollution in the city of Blantyre, Malawi: lead, zinc and cadmium. Proceedings of the first Chancellor College Research Dissemination Conference 28 – 30 March 2001, University of Malawi: Zomba, 317 – 321.

Mataka, L.M., Henry, E.M.T., Masamba, W.R.L and Sajidu, S.M (2006). Lead remediation of contaminated water using Moringa Stenopetala and Moringa oleifera seed powder. *International Journal of Environmental Science and Technology*, 3(2): 131-139.

Matope, J (2002). Blantyre City Environmental Profile report. United Nations Development Programme, Geneva.

McBride, M.B (1994). Environmental chemistry of soils. Oxford University Press, New York, 154 – 165.

Meir, L.P and Kahr, G (1999). Determination of the cation exchange capacity (CEC) of clay mineral using the complexes of copper (II) ion with triethylenetetramine and tetraethylenepentamine. *Clays and Clay Minerals*, 47: 386-388.

Mier, M.V., Callejas R.L., Gehr, R., Cisnero B.E.J and Alvarez P.J.J (2001). Heavy metal removal with Mexican clinoptilolite: multi-component ionic exchange. *Water Research*, 35(2) 373-378.

Mineralogy Database (2006). Corundum. <a href="http://webmineral.com/data">http://webmineral.com/data</a>

Molla-Abbassi, A., Eriksson, L., Mink, J., Persson, I., Sandström, M., Skripkin, M., Ullström, A.-S and Lindqvist-Reis, P (2002). Structure and bonding of bisaquamercury(II) and

trisaquathallium(III) trifluoromethanesulfonate. *Journal of the Chemical Society, Dalton Transactions*, 4357-4364.

Monteiro, M.I.C., Ferreira, F.N., de Oliveira, N.M.M and Avila, A.K (2003). Simplified version of the sodium salicylate method for analysis of nitrate in drinking waters. *Analytica Chimica Acta*, 477: 125-129.

Morton, J.F (1991). The horseradish tree, Moringa Pterygosperma (Moringaceae). *Economic Botany*, 43 (3): 318-333.

Muyibi, S.A (1994). The potential of Zogale (Moringa oleifera) seeds as a water treatment chemical. *Nigerian Society of Engineers*, 29 (1): 27-33.

Muyibi, S.A., Noor, M.J.M.M., Leong, T.K and Loon, L.H (2002). Effect of oil extraction from Moringa oleifera seeds on coagulation of turbid water. *Environmental Studies*, 59 (2): 243-254.

Muyibi, S.A and Alfugara, A.M.S (2003). Treatment of surface water with Moringa extract and Alum – A comparative study using a pilot scale water treatment plant. *International Journal of Environmental Studies*, 60 (6): 617-626.

Ndabigengesere, A., Narasiah, K.S and Talbot B. G (1995). Active Agents and Mechanism of Coagulation of Turbid Waters using Moringa Oleifera. *Water Research*, 29 (2): 703-710.

Ndabigengesere A and Narasiah K.S (1998). Quality of water treated by coagulation using Moringa Oleifera seeds. *Water Research*, 32 (3): 781-791.

Nishio, H., Hayashi C., Lee M.J., Ayaki, H, Yamamoto, R., Ninomiya, R., Koisumi, N and Sumino, K (1999). Itai-itai disease is not associated with polymorphism of the estrogen receptor α gene. *Archives of Toxicology*, 73: 496-498.

Okuda, T., Baes, A.U., Nishijima, W and Okada, M (2001). Coagulation mechanism of salt solution extracted active component in Moringa oleifera seeds. *Water Research*, 35 (3): 830 – 834.

Omae, A., Solo-Gabriele, H and Townsend, T (2006). A chemical stain for identifying arsenic-treated wood. Report No. 05-0432025, State university of Florida, Florida Center for solid and hazardous waste management, 7-8.

Pehlivan, E and Altun, T (2007). Ion-exchange of Pb<sup>2+</sup>, Cu<sup>2+</sup>, Zn<sup>2+</sup>, Cd<sup>2+</sup> and Ni<sup>2+</sup> ions from aqueous solution by Lewatit CNP 80. *Journal of Hazardous Materials*, 140: 299-307.

Pleysier, J and Cremers, A (1975). Stability of silver-thiourea complexes in montmorillonite clay. *Faraday Transactions*, 71: 256 – 264.

Pollard, S.J.T., Thompson, F.E and McConnachie, G.L (1995). Microporous carbons from Moringa oleifera husks for water purification in less developed countries. *Water Research*, 29 (1): 337-347.

Pratt, J.H., Henry, E.M.T., Mbeza, H.F., Mlaka, E and Satali L.B (2002). Malawi Agroforestyry Extension Project Marketing & Enterprise Program. Main Report, Malawi Agroforestry, Publication No.47, 53-62.

Price, M. L (2000). The Moringa Tree. Echo technical note. http://www.echonet.org

Richter, N., Siddhuraji, P and Becker, K (2003). Evaluation of nutritional quality of moringa (Moringa oleifera Lam.) leaves as an alternative protein source for Nile tilapia (Oreochromis niloticus L.). *Aquaculture*, 217: 599-611.

Rhoades, J.D (1982). Cation exchange capacity. pp. 149-157. *In* Page A.L (ed.) '*Methods of soil analysis. Part 2: Chemical and Microbiological properties*' Second Edition, ASA and SSSA, Madison, WI.

Rossi, A., Poverini, R., Di Lullo, G., Modesti, A., Modica, A and Scarino, M.L (1996). Heavy metal toxicity following apical and basolateral exposure in the human intestinal cell line Caco-2. *Toxicology in Vitro*, 10: 27-36.

Roundhill, D.M (2004). Novel strategies for removal of toxic metals from soils and waters. *Journal of Chemical Education*, 81(2): 275-282.

Scoog, D.A., West, D.M., Holler, F.J and Crouch, S.R (2004). Fundamentals of analytical chemistry. 8<sup>th</sup> Edn, Thomson Brooks/Cole: Belmont, 708-868.

Serrano, S., Garrido, F., Campbel, C.G and Garcia-Gonzalez, M.T (2005). Competitive sorption of cadmium and lead in acid soils of Central Spain. *Geoderma*, 124: 91-104.

Sharma, P., Kumari, P., Srivastava M.M and Srivastava, S (2007). Ternary biosorption studies of Cd(II), Cr(III) and Ni(II) on shelled Moringa oleifera seeds. *Bioresource Technology*, 98 (2): 474-477.

Shriver, D. F., Atkins, P. W and Langford, C. H (1992). Inorganic Chemistry. Oxford University Press, Oxford, 173-174.

Silva, D.L and Brunner, G (2006). Desorption of heavy metals from ion exchange resin with water and carbon dioxide. *Brazilian Journal of Chemical Engineering*, 23 (2): 213-218.

Simpson, C and Laurie, S.H (1999). Ion exchange studies on zinc-rich waste liquors. *Hydrometallurgy*, 51 (3): 335-344.

Singh, S.P., Ma, L.Q and Harris, W.G (2001). Heavy metal interactions with phosphatic clay: sorption and desorption behaviour. *Journal of Environmental Quality*, 30: 1961-1968.

Sofowora, A (1993). Medicinal Plants and Traditional Medicine in Africa. 2<sup>nd</sup> Edn. Spectrum Books Limited, Ibadan, 285 pp.

Soliva, C.R., Krenzer, M., Foidl, N., Foidl, G., Machuller, A and Hess, H.D (2005). Feeding value of whole and extracted Moringa oleifera leaves for ruminants and their effects on ruminal fermentation in vitro. *Animal Feed Science and Technology*, 118: 47-62.

Stahl, R., Jacobs, H (1997). Zur Kristallstruktur von Sr[Zn(OH)<sub>4</sub>]·H<sub>2</sub>O. Zeitschrift fur Anorganische und Allgemeine Chemie, 623: 1273-1276.

Stumm, W (1992). Chemistry of the solid water interface: processes at the mineral-water and particle-water interface in natural systems. John Wiley: New York, 13-39.

Sutherland, J.P., Folkard, G.K., Mtawali, M.A and Grant W.D (1994). *Moringa oleifera* as a natural coagulant. 20<sup>th</sup> WEDC Conference, Affordable Water Supply and Sanitation, Colombo, Sri Lanka, 297-299.

Tahiliani, P and Kar, A (1999). Role of Moringa oleifera leaf extract in the regulation of thyroid hormone status in adult male and female rats. *Pharmacological Research*, 41 (3): 319-323.

Takamatsu, R., Asakura, K., Chun, W.J., Miyazaki, J and Nakano, M (2006). EXAFS studies about the sorption of cadmium ions on montmorillonite. *Chemistry Letters*, 35 (2): 224 – 225.

Takeuchi, Y and Arai, H (1990). Removal of coexisting Pb<sup>2+,</sup> Cu<sup>2+</sup> and Cd<sup>2+</sup> ions from water by addition of hydroxyapatite powder. *Journal of Chemical Engineering of Japan*, 23 (1): 75-80.

Tanner, M.S (1998). Role of copper in Indian Childhood Cirrhosis. *American Journal of Clinical Nutrition*, 67: 1074S-1081S.

Thompson, A., Attwood, D., Gullikson, E., Howells, M., Kim, K.J., Kirz, J., Kortright, J., Lindau, I., Pianatta, P., Robinson, A., Scofield, J., Underwood, J., Vaughan, D., Williams, G., Winick, H (2001). X-ray Data Booklet, LBNL/PUB-490 Rev. 2, Lawrence Berkeley National Laboratory, Berkeley, California 94720.

Voronin, V. A., Shchennikov, V. V., 1989. Change of structure of mercury oxide under the action of pressure. *Kristallografiya*, 34: 491-493.

Walstad, D (2003). Ecology of the planted aquarium. 2<sup>nd</sup> Edn, Echnodorus Publishing, Chapel Hill, NC, 194 pp.

Warhust, A.M., McConnachie, G.L and Pollard, S.J.T (1997a). Characterization and applications of activated carbon produced from Moringa oleifera seed husks by single-step steam pyrolysis. *Water Research*, 31 (4): 759-766.

Warhust, A.M., Fowler, G.D., McConnachie, G.L and Pollard, S.J.T (1997b). Pore structure and adsorption characteristics of steam pyrolysis carbon from Moringa oleifera. *Carbon*, 35 (8): 1039-1045.

Warhust, A.M., Ragget, S.L., McConnachie, G.L., Pollard S.J.T., Chipofya, V and Codd, G.A (1997c). Adsorption of the cyanobacterial heptatotoxin microcystin-LR by a low – cost activated carbon from the seed husks of the pan-tropical tree, Moringa oleifera. *The Science of Total Environment*, 207: 207-211.

WHO, World Health Organization, (2004). Guidelines for drinking water quality. 3<sup>rd</sup> Edn. Vol. 1, Recommendations, WHO: Geneva, 296-459

Williamson, J (1975). Useful Plants of Malawi. University of Malawi, Zomba: Malawi, 163.

Yang, J.E., Skogley, E.O., Schaff, B.E and Kim, J.J (1998). A simple spectrophotometric determination of nitrate in water, resin, and soil extracts. *Soil Science Society of America Journal*, 62: 1108-1115.

### **APPENDICES**